Allostery in Caspases

by

Debajyoti Datta

DISSERTATION

Submitted in partial satisfaction of the requirements for the degree of

DOCTOR OF PHILOSOPHY

in

Biophysics

in the

GRADUATE DIVISION

of the

UNIVERSITY OF CALIFORNIA, SAN FRANCISCO

Acknowledgements

For the last five years at UCSF, I have had the good fortune of being a part of the research group of Professor Jim Wells. The science during this time has certainly been interesting and intellectually engaging, but even more importantly, I have been surrounded by a number of incredibly talented and exciting scientists who have had a formative impact on my own development as a scientist. These people were instrumental in helping me with the work presented in this dissertation, and I would like to thank them here.

First and foremost, I would like to thank my advisor and mentor, Professor Jim Wells, for giving me the opportunity to join his research group. When I first came to Jim to ask to rotate in his lab, he had arrived at UCSF all of a few weeks before, and he initially hesitated to have me in the lab before it was finished being setup. Luckily for me, we found a project that I could begin working on immediately. Since then I have benefitted tremendously from his mentorship and scientific insight in my field of study. I am especially appreciative of his dedication to training future scientists, the support and encouragement he has given me over the years, and his infectious excitement about my own work, even when things slowed down. From Jim, I have learned the joy of being on the cutting edge of scientific discovery.

I am also deeply indebted to the many post-docs and graduate students that I have worked closely with while in graduate school. My rotation project was a continuation of a research project begun by Dr. Justin Scheer, who supervised me during my first year. Thanks to him I had a smooth transition into the lab and I was able to hit the ground running on a project that would eventually turn into my thesis studies. Dr. Junjun Gao joined the Wells lab shortly after I did, and he was my partner in crime on the inflammatory caspases for much of my time with the group. I would also like to thank Dr. Dennis Wolan for his expertise as our resident

structural biologist and for instilling a sense of discipline in the lab so that other post docs would not have to. I appreciate the many insightful discussions I had with Dr. Sami Mahrus both on my project and during my preparation for my oral exam. I would also like to thank Dr. Jack Sadowsky for his guidance when I decided to get my hands wet with some chemistry, and Dr. Nick Agard for his time and effort in helping me with cell culture work. I am especially thankful to Julie Zorn, a fellow graduate student, for her colorful sense of humor, numerous practical jokes, and for her teamwork in keeping the Wells group post docs in line.

Our lab would likely cease to function without the expert support of Mary Betlach and Marja Tarr. Since the day I walked into the Wells lab, Mary has been instrumental in providing guidance and advice for numerous grant and fellowship applications, and I am indebted to her for the help she gave me in securing my graduate fellowships. Marja and I have become great friends in our time together with the Wells group, and she has been invaluable not only with scheduling and ordering issues, but also always having candy around to satisfy my sweet tooth and being there to listen.

Professor Charly Craik and Professor Robert Fletterick served on both my thesis committee and my oral examination committee, and I especially thankful to them for their advice and guidance on this project. I would also like to thank Professor John Gross, who served as the chair of my oral examination committee and gave me a tremendous amount of constructive feedback on my proposal. Professor Art Weiss was the last member of my orals committee, and I appreciate his time and advice for my project. Professor Weiss was also the director of the Medical Scientist Training Program, and I am thankful for his dedication to the program and for accepting me when I applied here. I don’t think my parents will ever forget the

message Professor Weiss left on their answering machine eight years ago informing us of my acceptance to the UCSF MSTP.

My training in graduate school would not have been possible without the extensive support of the both the MSTP and the Biophysics Program. Professor Kevin Shannon is the current director of the MSTP and I am grateful for his efforts in working with the various administrations at UCSF to smooth our transitions over the course of our training. Jana Toutolman and Catherine Norton at the MSTP office are also terrifically dedicated to the program and our well being, and I am thankful for all of their help and support over the last seven years at UCSF, and two more to come. I would also like to express my appreciation to Julie Ransom and Rebecca Brown in the Biophysics office, who have been my advocates with the graduate program for the last five years and have helped make graduate school such a terrific experience.

I would also to thank my funding sources that supported me during graduate school. This includes the National Institute of Health through its support of our MSTP, and fellowships from the American Heart Association and University of California Cancer Research Coordinating Committee.

The last five years of graduate school have been a formative time for me not only as a scientist, but also as a human being. I owe my well being to a small but fantastic group of friends that have been with me for almost seven years. The best part about coming to UCSF for my training has been meeting the other nine members of my MSTP class, Ahnika Kline, Amy Chang, Beth Apsel, Cathy Collins, Davina Wu, Ervin Johnson, Jay Gardner, Sarah Morton, and Trung Pham. In them I know I have found life-long friends who will share in all that my future holds.

Beth has been one of my closest friends since the first months of medical school, and it was wonderful being able to talk with her multiple times a day, every day, through our time in graduate school together. When I first met Ervin, I was scared of him and never would have guessed we would end up friends, but graduate school would have been very different without having him around for lunch and trips to the gym nearly every day. Trung, my friend and roommate since my second day in California, has become like a brother to me during our time here. I regret missing out on meeting Jay in college, so I am very thankful that we have become such great friends during our time here. Though I may never forgive Brian Berger for stealing Amy away from our household, I couldn't imagine life without his friendship since the beginning of medical school. I must also thank Amy and Brian for Penny and Jack. I am very grateful to my roommate Marisol Peneloza for keeping it crazy. Matt Callahan has been my roommate for longer than anyone. After three years in college and six years in San Francisco, there may be some legal obligations between us, I'm not sure. I thank him for his long time friendship and his flexibility in scheduling our Treks around my whims.

This Dissertation is dedicated to my Mom and Dad. I have known only unconditional love and support from them for as long as I can remember. Whatever my successes or failures, I am blessed to have them behind me for every step on this journey.

Chapter Specific Acknowledgements

All of the work presented in this dissertation was performed under the direct supervision of Professor James A. Wells. Additional contributions to specific chapters are described below.

Chapter 2 was previously published: Datta D, Scheer JM, Romanowski MJ, Wells JA. (2008) "An allosteric circuit in caspase-1." *Journal of Molecular Biology*. 381(5): 1157-67. The original plan to target residues for mutagenesis in section 2.2 was laid out by Dr. Justin Scheer. The creation of clones for salt bridge variants in section 2.3 and crystallography screening, data collection, and refinement for the three structures presented were carried out by Dr. Justin Scheer and Dr. Michael Romanowski.

Chapter 3 of this dissertation is being prepared for publication. The design scheme for constructing half-labeled caspase constructs was devised by Dr. Scheer and Professor Wells, and Figure 3.3 was created by Dr. Scheer. The plan to generate the G287A and P343A mutants in section 3.6 was laid out by Dr. Scheer. Dr. Junjun Gao developed the conformation-specific antibodies used in section 3.7 and that work was published: Gao J, Sidhu SS, Wells JA. (2009) "Two-state selection of conformation-specific antibodies." *Proceedings of the National Academy of Sciences* U S A. 106(9):3071-6.

The experiments in section 4.2 on engineering a caspase-7 salt bridge were designed by Dr. Scheer, and the clones for caspase-7 mutant constructs were made by him. The future studies proposed in section 4.3 on studying caspase processivity were presented as part of my Orals Proposal. The cell culture work and media collection for the experiments presented in section 4.4 were done by Dr. Scheer.

Allostery in Caspases

Debajyoti Datta

Abstract

Caspases are a family of dimeric thiol proteases central to the inflammatory and apoptotic pathways. Structural studies of the major inflammatory caspase, caspase-1, reveal that the enzyme exists in two states: an on-state when the active site is occupied; or an off-state when the active site is empty or when the enzyme is bound by allosteric ligand at the dimer interface. Determining which residues and regions of the enzyme are responsible for determining enzyme conformation and for regulating transitions between states would elucidate the molecular basis for allostery in caspase-1.

A network of 21 hydrogen bonds from 9 side chains connecting the active and allosteric sites change partners when going between the on- and off-states. Alanine-scanning mutagenesis of these 9 side chains shows that only two of them, Arg286 and Glu390, which form a salt bridge, have major effects causing 100- to 200- fold reductions in catalytic efficiency (k_{cat}/K_M). More detailed mutational analysis reveals that the enzyme is especially sensitive to substitutions of the salt bridge: a homologous R286K substitution causes a 150-fold reduction in k_{cat}/K_M. Thus, side chains from only a small subset of the larger H-bonding network are critical for activity. These form a contiguous set of interactions that run from one active site through the allosteric site at the dimer interface and on to the second active site. This subset constitutes a functional allosteric circuit or “hot-wire” that promotes site-to-site coupling.

Further experiments demonstrate the utility of using site-directed mutagenesis and chemical ligands to select for and examine enzyme conformation. Targeting specific glycine and proline residues in caspase-1 for mutation selects for different conformational states of the enzyme. We present a method of using covalent inhibitors for caspases to create half-labeled

hybrid constructs that trap the conformational state of caspases in solution and allow us to understand how allostery plays a role in caspase activity. We present a model that provides a mechanism by which the very conformational state of the various caspase family members recapitulates their role in specific biologic pathways and provides an additional level of regulation.

Table of Contents

List of Tables

List of Figures

List of Abbreviations

β-ME	2-Mercaptoethanol
Ac-DEVD-AFC	Ac- Asp-Glu-Val-Asp -7-Amino-4-trifluoromethylcoumarin
Ac-WEHD-AFC	Ac-Trp-Glu-His-Asp-7-Amino-4-trifluoromethylcoumarin
Apaf-1	apoptosis protease-activating factor-1
ASC	apoptosis-associated speck-like protein containing a CARD
ATCase	aspartate transcarbamoylase
ATP	adenosine-5'-triphosphate
β-ME	2-Mercaptoethanol
CARD	caspase recruitment domain
CBP	CREB-binding protein
COP	CARD-only protein
CREB	cAMP response element–binding protein
CTL	cytotoxic T-lymphocyte
DABCYL	4-(dimethylaminoazo)benzene-4-carboxylic acid
DAMP	danger-associated molecular pattern
DED	death effector domain
DEVD	Asp-Glu-Val-Asp
DISC	death-inducing signaling complex
DNA	deoxyribonucleic acid
DTT	DL-dithiothreitol
EDANS	(5-((2-Aminoethyl)amino)naphthalene-1-sulfonic acid)
EDTA	ethylenediaminetetraacetic acid
ELISA	Enzyme-linked immunosorbent assay

Fab	fragment antigen-binding
FADD	Fas-associated death domain
FasL	Fas ligand
FRET	Förster resonance energy transfer
GTP	guanosine-5'-triphosphate
HDAC	Histone deacetylase
HEPES	4-(2-hydroxyethyl)-1-piperazineethanesulfonic acid
ICE	interleukin-1β converting enzyme
IL	interleukin
IL-1β	interleukin-1β
IL-1ra	IL-1 receptor antagonist
IPAF	ICE-protease activating factor
IPTG	Isopropyl β-D-1-thiogalactopyranoside
KSHV	Kaposi's sarcoma associated herpesvirus
LC-MS	liquid chromatography-mass spectrometry
LPS	lipopolysaccharide
LRR	leucine rich repeat
MAP	mitogen-activated protein (kinase)
MSU	monosodium urate
MWC	Monod-Wyman-Changeux
MWCO	molecular weight cut-off
NACHT	domain present in NAIP, CIITA, HET-E, and TP1
NAIP	neuronal apoptosis inhibitory protein
NALP	NACHT-, LRR- and PYD-containing protein
N-CoR	nuclear receptor corepressor

NF-κB	nuclear factor kappa-light-chain-enhancer of activated B cells
NK	natural killer (cells)
NLRP	NACHT, LRR and PYD domains-containing protein
NMR	nuclear magnetic resonance
Nod1	nucleotide-binding oligomerization domain-containing protein 1
Nod2	nucleotide-binding oligomerization domain-containing protein 2
NLR	Nod-like receptors
PAMP	pathogen-associated molecular pattern
PEG MME	Polyethylene glycol monomethyl ethers
PI-9	proteinase inhibitor 9
PIPES	1,4-Piperazinediethanesulfonic acid
PRM	pattern receptor molecule
PYD	pyrin domain
RNA	ribonucleic acid
SPR	surface plasmon resonance assay
TLR	Toll-like receptors
TNF	tumor necrosis factor
TRAIL	TNF-related apoptosis-inducing ligand
VAD-FMK	Val-Ala-Asp-fluoromethylketone
VEGF	vascular endothelial growth factor
WEHD	Trp-Glu-His-Asp

Chapter 1:

Introduction to caspases and allostery

1.1 The caspase family of proteases

The caspases comprise a related family of proteases (11 in humans) that have central roles in apoptosis and inflammation. The name "caspase" is a contraction of "cysteine-dependent aspartate-specific protease" (Alnemri, Livingston et al. 1996). These proteases are dependent on an active site cysteine side chain for catalyzing peptide bond cleavage, and as a family show high specificity for cleaving peptide substrates following an aspartate residue (Shi 2002). Whereas the use of a nucleophilic cysteine side chain is found in several protease families, the primary specificity for aspartate is in fact quite rare among proteases; granzyme B, a serine protease which itself activates caspase, is the only other known mammalian protease to share this specificity for aspartate (Timmer and Salvesen 2007). Caspases are almost always found to be associated with specific signaling events, and are rarely associated with non-specific degradation of proteins. Downstream signals are conveyed by limited cleavage of specific substrates to activate a given pathway (Pop and Salvesen 2009).

Historically, the members of the caspase family have been classified as either "pro-inflammatory" or "apoptotic" based on their presumed role in cellular processes and sequence similarity. The apoptotic caspases are further categorized as either "initiator" (caspase-2, -8, -9, and -10) or "executioner (caspase-3, -6, -7). Despite their designation, the pro-inflammatory caspases (caspase-1, -4, -5) have also been implicated in a form of programmed cell death termed "pryoptosis" that is associated with massive activation of inflammatory cells (Labbe and Saleh 2008). Human caspases are widely expressed in a variety of tissues and cell types, with the exception of caspase-14, whose expression and function appears to be limited to keratinocyte differentiation (Denecker, Hoste et al. 2007).

Because of the increasing number of roles that caspases appear to be involved in that fall outside this classification scheme, an alternative classification scheme involves dividing the caspase family members according to the length of their N-terminal prodomains. In this scheme, the caspases are divided into initiator caspases (caspase-1, -2, -4, -5, -8, -9, -10) and effector caspases (-3, -6, -7). Initiator caspases have long prodomains containing one of two characteristic protein-protein interaction motifs; either the caspase recruitment domain (CARD) or the death effector domain (DED). These domains allow the caspases to interact with upstream adaptor molecules. The effector caspases have short prodomains and are responsible for cleaving multiple cellular substrates after being activated by upstream caspases (Li and Yuan 2008). We will use the older historical classification here, but it is important to note that growing evidence suggests that the apoptotic initiator caspases are more closely related to inflammatory caspases than to executioner caspases in terms of structure, activation mechanisms, and regulation.

1.2 Caspase-1 and the inflammatory caspase pathway

Caspase-1 is the best studied inflammatory caspase and the first member of the caspase family to be identified in humans. It is the protease responsible for processing prointerleukin-1β to its active form, interleukin-1β (IL-1β) (Black, Kronheim et al. 1989; Thornberry, Bull et al. 1992). Caspase-1 has also been identified as being involved in the activation of IL-18 and IL-33 (Gu, Kuida et al. 1997; Schmitz, Owyang et al. 2005). As such, caspase-1 is a central driver of inflammation and a major player in the innate immune response. In addition to caspase-1, two other human caspases, caspase-4 and caspase-5, are involved in regulating inflammation (Petrilli, Dostert et al. 2007). In this section we review recent work in defining the components

of the inflammatory pathway that lead to caspase-1 activation. We also discuss various pathologies associated with disregulation of this system and current approaches to development of therapies targeting caspase-1 and IL-1β signaling.

1.2.1 Components of the inflammatory signaling pathway

The inflammatory caspases are central mediators of the innate immune response. Innate immunity allows the body to rapidly respond to microbial "pattern" molecules that differentiate pathogens from the host, such as components of the bacterial cell wall. These pattern molecules, often referred to as pathogen-associated molecular patters (PAMPs) (Janeway and Medzhitov 2002), are recognized by germline-encoded pattern receptor molecules (PRMs), which include the Toll-like receptors (TLRs) and Nod-like receptors (NLRs) (Martinon and Tschopp 2005). Interestingly, this same pathway that cells use to detect the presence of foreign pathogens can also be used to detect endogenous danger or stress signals termed danger-associated molecular patterns (DAMPs) (Petrilli, Dostert et al. 2007).

TLR family members are membrane-associated receptors that sense extracellular ligands and trigger a signaling cascade that leads to the expression of immune and inflammatory genes (Church, Cook et al. 2008). There are 10 TLRs in humans (O'Neill 2006), including TLR4 which senses lipopolysaccharide (LPS), a outer membrane component of gram-negative bacteria (O'Neill 2008). Sensing of a danger signal leads to activation of two major pathways; the first involves the transcription factor NF-κB, a master switch of inflammation, and the second involves activation of the MAP kinase pathway (O'Neill 2006).

The NLR family of PRMs includes 22 members in humans (Schroder and Tschopp 2010). These proteins are the cytoplasmic counterparts of the TLR family, and detect PAMPs that gain access to the interior of the cell, as well as various metabolic stresses (Church, Cook et al. 2008). Various members of the NLR family activate host signaling pathways in different ways. Nod1 and Nod2 were some of the first NLRs to be identified and these PRMs sense bacterial molecules that are components of peptidoglycan in bacterial cell walls. In response to these agonists, Nod1 and Nod2 induce activation of NF-κB and the MAP kinase pathway, similar to TLR signaling. In contrast, other members of the NLR family such as a NLRP3 (also called cryopyrin or NALP3), NLRC4 (also called IPAF), and NLRP1 (also called NALP1) are scaffolding proteins that are involved in the assembly of multiprotein complexes called "inflammasomes" (Franchi, Eigenbrod et al. 2009). These complexes are thought to be the main site for inflammatory caspase recruitment and activation. Most of the work on NLR proteins and inflammasomes has been done in the context of caspase-1. Consequently, it is currently unknown which components of the NLR family are able to activate caspase-4, but caspase-5 has been shown to be activated by NLRP1 (Petrilli, Dostert et al. 2007).

A diverse number of PAMPs and DAMPs have been found to activate the caspase-1 pathway following recognition of these patterns by the TLRs and NLRs. These activators include bacterial toxins, lipopolysaccharide, bacterial RNA, flagellin, uric acid crystals, and UVB radiation (Petrilli, Dostert et al. 2007). Perhaps the best studied caspase-1 activation pathway involves NLRP3, which is the only NLR that has been shown to respond to both PAMPs and DAMPs. Exposing cells to high concentrations of the DAMP ATP leads to activation of P2X7 ion channel receptors that open to cause a rapid cellular efflux of potassium. The resulting caspase-1 activation is dependent on the presence of NLRP3 and ASC (Mariathasan, Weiss et al. 2006). It is still not well understood how sensing of various PAMPs and DAMPs by the cell leads to NLRP3

activation, and several models explaining the mechanism are still hotly debated, but recent reports suggest that the formation of reactive oxygen species may be a central component to various activation pathways (Schroder and Tschopp 2010).

A complete understanding of the various pathways in which caspase-1 can be activated remains to be elucidated. However, a common feature of all these pathways appears to be recruitment of procaspase-1 by multiprotein complexes containing NLRs and subsequent proteolytic processing leading to activation. Active caspase-1 is then able to cleave and activate pro-IL-1β, which is secreted by the cell as an inflammatory cytokine that activates other immune cells. IL-1β, along with tumor necrosis factor (TNF)-α and vascular endothelial growth factor (VEGF), is a central pro-inflammatory cytokine. One of the main functions of IL-1β is its role as a pyrogenic cytokine. Even at low concentrations, it causes fever, hypotension, and induces the production of other inflammatory cytokines. IL-1β is produced in a variety of settings, including infection, immunologic challenge, and injury (Church, Cook et al. 2008).

1.2.2 Pathologies associated with the caspase-1/IL-1β inflammatory pathway

Excessive caspase-1 activity and IL-1β production can lead to a variety of pathologies including septic shock and gout (Joshi, Kalvakolanu et al. 2002; Martinon, Petrilli et al. 2006). The dangers of excessive or dysregulated IL-1β signaling are reflected by the number of proteins that have evolved to regulate IL-1β production by the caspase-1 pathway. These include proteins that contain a CARD domain, such as the CARD-only protein (COP), ICEBERG, proteinase inhibitor 9 (PI-9), and pyrin. These are thought to regulate IL-1β production by interfering with caspase-1 activity or its recruitment to inflammasomes (Church, Cook et al. 2008)

The crystal-induced inflammatory diseases gout and pseudogout result in activation of macrophages and neutrophils in joints. Both of these conditions are dependent on the sensing of monosodium urate (MSU, in gout) and calcium pyrophosphate dehydrate (in pseudogout) crystals by the NLRP3 inflammasome and subsequent IL-1β signaling (Martinon, Petrilli et al. 2006). MSU is also released from necrotic cells, and the subsequent inflammatory response to necrosis is dependent on this same pathway (Shi, Evans et al. 2003).

A variety of inflammatory disorders are characterized by dysregulation of the caspase-1/IL-1β pathway, and these diseases can be thought of as being either autoimmune or autoinflammatory. Autoimmune disorders (such as rheumatoid arthritis, inflammatory bowel disease, type 1 diabetes, psoriasis, lupus, and multiple sclerosis) are processes driven by auto-reactive T-cells, where the inflammatory component is secondary to the primary, dysfunctional T cell. Therefore, treatments that attempt to modulate the caspase-1/IL-1β pathway may provide symptomatic relief of inflammation in autoimmune disorders without affecting the underlying cause of the disease (Dinarello 2010). For example, blocking IL-1 receptors or neutralizing IL-1β has been effective in protecting bone and cartilage in rheumatoid arthritis. In contrast, autoinflammatory diseases do not involve T cells and therefore are not mediated by the adaptive immune system. Rather, the primary actors of disease are dysfunctional macrophages that are driven by excess stimulation with IL-1β. As a result, in autoinflammatory disorders, targeting the caspase-1/IL-1β pathway is central to treatment of disease (Dinarello 2010).

Mutations in the NLRs are a common cause of inflammatory diseases. Activating mutations in Nod2 are associated with Crohn's disease and Blau syndrome (Hugot, Chamaillard et al. 2001; Miceli-Richard, Lesage et al. 2001; Ogura, Bonen et al. 2001). Mutations in NLRP3

affect IL-1β processing (Hoffman, Mueller et al. 2001). In type 2 diabetes, a chronic state of IL-1β-driven inflammation leads to destruction of the insulin producing β islet cells (Dinarello 2010). Blockade of IL-1β signaling by the use of IL-1 receptor agonist (IL-1Ra, also called anakinra) or a specific neutralizing monoclonal antibody to IL-1β has been shown to be beneficial in patients with this disease (Larsen, Faulenbach et al. 2007; Dinarello 2010).

There is mounting evidence that caspase-1 and its substrate, IL-1β, are important mediators of inflammation and ischemic tissue damage in the brain following stroke. IL-1β was the first cytokine to be identified to act on the brain. It is known as the "endogenous pyrogen" since it causes fever and shock when released systemically. Clinical studies have shown that IL-1β is expressed quickly in the brain following acute injury. Levels of mRNA rise within 15 minutes and protein levels within one hour. Increased levels of IL-1β are also found in post-mortem brain tissue and cerebrospinal fluid of stroke patients. Neutralizing IL-1β antibodies have been shown to reduce ischemic brain damage in rats (Rothwell 2003).

1.2.3 Therapeutic approaches to modulating the caspase-1/IL-1β inflammatory pathway

Targeting both the production and downstream effectors of IL-1β activity has proven to be useful therapeutically in animal models of stroke. Non-selective caspase inhibitors are neuroprotective, and ischemic brain damage in mice is reduced by deletion of the caspase-1 gene or overexpression of dominant negative caspase-1. IL-1 receptor antagonist (IL-1ra) is a naturally occurring protein related to IL-1β. It is a highly selective, competitive agonist that can block all known effects of IL-1β. When it is injected into cerebral ventricles following cerebral ischemia or brain trauma in mouse models, IL-1ra markedly reduces neuronal loss. In neonatal rats, IL-1ra reduces damage following focal, global, reversible, or permanent ischemia, cerebral

hemorrhage, and hypoxia/ischemia. Neutralizing antibodies to IL-1ra exacerbate ischemic brain damage. These studies all highlight the importance of the caspase-1/IL-1β inflammatory pathway in ischemic brain damage following stroke. Unfortunately, any of the current neuroprotective agents for stroke or traumatic brain injury that have been tested in clinical trials have either failed to show efficacy or caused unacceptable adverse effects. Consequently, no widely available, effective treatments for stroke or traumatic brain injury exist (Boutin, Kimber et al. 2003).

IL-1 signaling also appears to contribute to heart failure following myocardial infarction. Animal models have shown that the use of IL-1Ra to reduce IL-1 activity prevents detrimental remodeling of myocardial tissue following infarction (Abbate, Salloum et al. 2008). A recent placebo-controlled trial also showed that a two week treatment with IL-1Ra in addition to standard therapy following myocardial infarction led to improved heart function three months later (Abbate, Kontos et al. 2010).

Caspase-1 has been an attractive target in the pharmaceutical industry for the development of anti-inflammatory drugs. However, few caspase-1 active-site inhibitors have entered clinical trials. One, pralnacasan, was found to significantly reduce joint symptoms and inflammation in Phase II clinical trials for rheumatoid arthritis. However, the trials were discontinued due to liver abnormalities and an unfavorable toxicity profile, likely due to non-selective caspase inhibition. One significant problem with these active site compounds is that they contain an electrophilic warhead and an aspartyl functionality, reducing their bioavailability and cell permeability (O'Brien, Fahr et al. 2005). As a result of the non-specific and highly reactive nature of current drugs, the active site of caspase-1 remains an attractive but

chemically elusive target for drug discovery. Therefore, better understanding of allosteric regulation in caspase-1 may lead to alternate therapeutics for a variety of disorders.

1.3 Apoptosis and apoptotic caspases

Kerr, Wylie, and Currie coined the term "apoptosis" in 1972 to describe a mode of cell death characterized by fragmentation of genomic DNA, the breaking up of a cell into a number of membrane-bound fragments, and the shedding of "apoptotic bodies" that are phagocytosed by other cells (Kerr, Wyllie et al. 1972). In the almost 40 years since then, the molecular mechanisms of this process have been widely studied. Apoptosis is a mechanism of cell death unique to multicellular organisms that permits removal of unwanted cells in a manner that is safe and controlled for neighboring cells and the entire organism. During this process, hundreds of proteins in the cell are subjected to restricted proteolysis (Luthi and Martin 2007; Mahrus, Trinidad et al. 2008). The principle proteases responsible for this are caspases.

1.3.1 The role of caspases in apoptosis

Apoptotic caspases are normally present in healthy cells as inactive precursors with little protease activity. Various mechanisms leading to caspase activation and subsequent apoptosis have been worked out, but a central feature of all pathways is the activation of executioner caspases, caspase-3, -6, or -7. These are the proteases that appear responsible for cleaving the vast majority of substrates during apoptosis. The substrates include cytoskeleton components such as actin, tubulins, and intermediate filament proteins whose cleavage likely causes the rounding of cells seen in early stages of apoptosis; nuclear lamins whose cleavage leads to

fragmentation of the nuclear envelope and nucleus; housekeeping proteins such as transcription and translation factors; inhibitory factors of DNase whose activation leads to degradation of genomic DNA; and numerous others (Taylor, Cullen et al. 2008).

The controlled process of cell removal in apoptosis is central to the well being of multicellular organisms. The other major mechanism by which cells can die is necrosis, or uncontrolled cell death. Necrotic events are characterized by the rapid disintegration of the cellular membrane and release of intracellular contents into the extracellular space. The presence of intracellular components in the extracellular space represents a large number of DAMPs that can be sensed by inflammatory cells of the innate immune system (reviewed above). Therefore, apoptosis allows cells to die without triggering potentially harmful inflammation in the surrounding tissue (Taylor, Cullen et al. 2008).

1.3.2 Activation pathways of caspases in apoptosis

Stimuli that induce apoptosis seem to do so through one of three major pathways. The first major pathway involves the sensing of internal cellular stresses such as heat shock, ionizing radiation, or cytotoxic chemicals that cause permeabilization of the mitochondrial membrane. This allows release of cytochrome c from the mitochondria into the cytosol, where it can bind to the scaffolding protein apoptosis protease-activating factor-1 (Apaf-1) and form the multiprotein complex known as the apoptosome. This complex is able to recruit and activate the initiator caspase caspase-9. Caspase-9 then initiates a proteolytic cascade by cleaving the executioner caspases-3 and -7 leading to apoptosis (Creagh, Conroy et al. 2003).

The second major apoptotic pathway involves the sensing of extracellular danger signals. The sensors responsible for transducing this signal across the cell membrane are a family of “death” receptors that are part of the TNF receptor superfamily. A variety of ligands have been identified that can stimulate these receptors, such as TNF, Fas ligand (FasL), and TNF-related apoptosis-inducing ligand (TRAIL), and this leads to oligomerization and conformational change of the receptors. Recruitment of adaptor molecules such as Fas-associated death domain (FADD) protein leads to formation of a multiprotein complex called the death-inducing signaling complex (DISC) akin to formation of the apoptosome. The DISC complex recruits the initiator caspase caspase-8. Caspase-8 then initiates a proteolytic cascade, either through the direct activation of executioner caspases or by cleavage of the protein Bid which can induce release of cytochrome c from the mitochondria and subsequent apoptosome formation (Creagh, Conroy et al. 2003).

Cytotoxic T-lymphocytes (CTLs) and natural killer (NK) cells are immune cells responsible for detecting and destroying virally infected and tumor cells, and they represent the third major pathway of apoptotic activation. CTLs and NK cells release cytolytic granules into their targets which contain the protease granzyme B, which is able to cleave and activate caspase-3, caspase8, and Bid, leading to apoptosis as described above (Creagh, Conroy et al. 2003).

Though activation of inflammatory caspases leads to a very different biological event in comparison to activation of apoptotic caspases, there are interesting parallels between the two activation pathways. Both involve sensing of danger signals, either intracellular or extracellular, and this leads to recruitment of scaffolding proteins to form multiprotein complexes. These complexes are then responsible for recruiting and activating caspase in both the inflammatory and apoptotic setting.

1.4 Caspase structure and function

Like many proteases, caspases are initially synthesized as zymogens, in this case a single chain polypeptide with an N-terminal prodomain. Maturation of caspase involves cleavage of the single chain into large and small subunits (20 kDa and 10 kDa, respectively, in caspase-1), which intimately associate to form the catalytic domain (Figure 1.1). In the case of initiator and inflammatory caspases, (such as caspase-8 or caspase-1, respectively) activation of the zymogen caspase is dependent on the dimerization step. On the other hand, executioner caspases, such as caspase-3, are active following the intrachain cleavage event (Garcia-Calvo, Peterson et al. 1999). The large subunit contains the cysteine and histidine that form the catalytic dyad, while the small subunit contributes additional residues to form the substrate binding pocket.

Structures of the active form of several caspases have been solved, and this has permitted identification of several key features of caspase structure (Figure 1.1, left). Homodimerization of caspases is mediated by hydrophobic interactions, with 6 anti-parallel β-strands from each monomer forming a single continuous 12 β-stranded sheet. The rest of the globular fold is filled out by several α-helices and short β-strands surrounding the central β-sheet. The two active sites of the caspase dimer are located on opposite ends of the central β-sheet and are formed by 4 protruding loops (L1-L4). L1 and L4 form the sides of the substrate binding groove and L3 forms the base. The catalytic cysteine is contained in L2 which crosses the groove. Among caspases, L1 and L3 have relatively conserved length and sequence, whereas L2 and L4 display greater variation which leads to different substrate specificities for various caspases (Riedl and Shi 2004).

Recently, a novel allosteric binding site was uncovered in the dimer interface of caspases approximately 15 Å from the active sites (Figure 1.1, right). This site is structurally

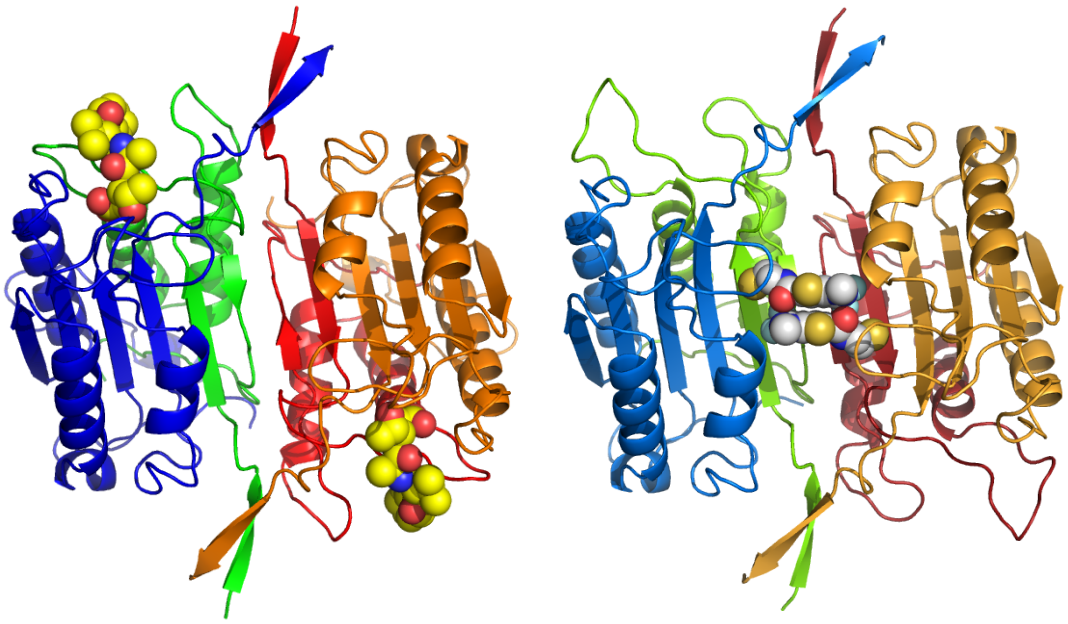

Figure 1.1. Crystal structures of the caspase-1 homodimer. Structures of wild type caspase-1 showing the domain structure of caspases. The dimer interface is in the center while the large subunits are colored blue and orange while the small subunits are colored green and red. **(Left)** Active site inhibitor z-VAD-FMK is bound in the active sites of each half of the dimer (yellow spheres, PDB ID code 2HBQ) **(Right)** Two molecules of an allosteric inhibitor are bound in the allosteric pocket at the dimer interface (white spheres, PDB ID code 2FQQ).

coupled to the active sites since binding in the dimer interface prevents peptide binding in the active site (Hardy, Lam et al. 2004; Scheer, Romanowski et al. 2006). Structural studies have shown that the compounds trap a natural off-state of mature caspase, suggesting that these proteases could be regulated via an allosteric mechanism by an unknown endogenous ligand (Scheer, Romanowski et al. 2006). Identification of such a ligand would reveal a new mechanism of regulation for pathways involving caspases and suggest novel therapeutic targets. More recent structural studies and modeling have suggested that binding of the intersubunit linker in the dimer interface may play a role in regulating the activation of procaspase-1 (Elliott, Rouge et al. 2009) and procaspase-3 (Walters, Pop et al. 2009).

1.5 Allostery

Since the determination of the first protein structure, studies have been undertaken to understand the mechanisms by which information is transmitted across large distances in proteins. This sort of "intramolecular signal transduction" is the purview of protein allostery, which can be broadly defined as how binding of a ligand at one site of a protein or macromolecular complex causes a modulation in catalytic efficiency or affinity at a distant site (Swain and Gierasch 2006).

The first systematic appraisal of allosteric enzymes was done by Monod and colleagues in 1965, where they proposed a framework for understanding allosteric transitions in proteins, which became to be known as the MWC, or concerted model (Monod, Wyman et al. 1965). Their model suggested that allosteric proteins are symmetric oligomers where each monomer can exist in one of at least two conformational states that have different affinities for ligands. The protein is able to interconvert between the two states in a concerted manner, but the oligomer cannot exist in a hybrid form. A competing model called the sequential model was later proposed by Koshland and colleagues that allowed for subunits of an allosteric protein to change conformation sequentially. Ligand binding to one subunit could alter its conformation without affecting neighboring subunits (Koshland, Nemethy et al. 1966). In subsequent years, further study on the ever expanding list of allosteric proteins has shown that it is likely that a variety of mechanisms are likely to exist by which allostery occurs, and more than one theoretical framework may be useful in understanding a given system (Gunasekaran, Ma et al. 2004).

In our discussion of caspases, we have described numerous studies that have revealed various properties of these proteases. The activation of caspases by recruitment to protein-

protein complexes, the regulation of caspases by binding partners, the identification of allosteric inhibitors to caspases; almost by definition, all of these properties point to the central importance of allosteric regulation in the caspase family of proteins.

1.6 Significance of research

The studies presented in this dissertation seek to uncover the molecular basis for allostery and positive cooperativity in caspase-1. We are interested in determining which residues or networks of residues are responsible for determining the conformational state of caspase-1 and regulating the transition between states. Further experiments seek to demonstrate the utility of using site-directed mutagenesis and chemical ligands to select for and examine conformational states of enzymes. These studies elucidate biophysical properties of caspase family members that reflect upon the biologic role of these proteases in their associated pathways.

1.7 References

Abbate, A., M. C. Kontos, et al. (2010). "Interleukin-1 blockade with anakinra to prevent adverse cardiac remodeling after acute myocardial infarction (Virginia Commonwealth University Anakinra Remodeling Trial [VCU-ART] Pilot study)." Am J Cardiol **105**(10): 1371-1377 e1.

Abbate, A., F. N. Salloum, et al. (2008). "Anakinra, a recombinant human interleukin-1 receptor antagonist, inhibits apoptosis in experimental acute myocardial infarction." Circulation **117**(20): 2670-83.

Alnemri, E. S., D. J. Livingston, et al. (1996). "Human ICE/CED-3 protease nomenclature." Cell **87**(2): 171.

Black, R. A., S. R. Kronheim, et al. (1989). "A pre-aspartate-specific protease from human leukocytes that cleaves pro-interleukin-1 beta." J Biol Chem **264**(10): 5323-6.

Boutin, H., I. Kimber, et al. (2003). "The expanding interleukin-1 family and its receptors: do alternative IL-1 receptor/signaling pathways exist in the brain?" Mol Neurobiol **27**(3): 239-48.

Church, L. D., G. P. Cook, et al. (2008). "Primer: inflammasomes and interleukin 1beta in inflammatory disorders." Nat Clin Pract Rheumatol **4**(1): 34-42.

Creagh, E. M., H. Conroy, et al. (2003). "Caspase-activation pathways in apoptosis and immunity." Immunol Rev **193**: 10-21.

Denecker, G., E. Hoste, et al. (2007). "Caspase-14 protects against epidermal UVB photodamage and water loss." Nat Cell Biol **9**(6): 666-74.

Dinarello, C. A. (2010). "Anti-inflammatory Agents: Present and Future." Cell **140**(6): 935-50.

Elliott, J. M., L. Rouge, et al. (2009). "Crystal structure of procaspase-1 zymogen domain reveals insight into inflammatory caspase autoactivation." J Biol Chem **284**(10): 6546-53.

Franchi, L., T. Eigenbrod, et al. (2009). "The inflammasome: a caspase-1-activation platform that regulates immune responses and disease pathogenesis." Nat Immunol **10**(3): 241-7.

Garcia-Calvo, M., E. P. Peterson, et al. (1999). "Purification and catalytic properties of human caspase family members." Cell Death Differ **6**(4): 362-9.

Gu, Y., K. Kuida, et al. (1997). "Activation of interferon-gamma inducing factor mediated by interleukin-1beta converting enzyme." Science **275**(5297): 206-9.

Gunasekaran, K., B. Ma, et al. (2004). "Is allostery an intrinsic property of all dynamic proteins?" Proteins **57**(3): 433-43.

Hardy, J. A., J. Lam, et al. (2004). "Discovery of an allosteric site in the caspases." Proc Natl Acad Sci U S A **101**(34): 12461-6.

Hoffman, H. M., J. L. Mueller, et al. (2001). "Mutation of a new gene encoding a putative pyrin-like protein causes familial cold autoinflammatory syndrome and Muckle-Wells syndrome." Nat Genet **29**(3): 301-5.

Hugot, J. P., M. Chamaillard, et al. (2001). "Association of NOD2 leucine-rich repeat variants with susceptibility to Crohn's disease." Nature **411**(6837): 599-603.

Janeway, C. A., Jr. and R. Medzhitov (2002). "Innate immune recognition." Annu Rev Immunol **20**: 197-216.

Joshi, V. D., D. V. Kalvakolanu, et al. (2002). "Role of caspase 1 in murine antibacterial host defenses and lethal endotoxemia." Infect Immun **70**(12): 6896-903.

Kerr, J. F., A. H. Wyllie, et al. (1972). "Apoptosis: a basic biological phenomenon with wide-ranging implications in tissue kinetics." Br J Cancer **26**(4): 239-57.

Koshland, D. E., Jr., G. Nemethy, et al. (1966). "Comparison of experimental binding data and theoretical models in proteins containing subunits." Biochemistry **5**(1): 365-85.

Labbe, K. and M. Saleh (2008). "Cell death in the host response to infection." Cell Death Differ **15**(9): 1339-49.

Larsen, C. M., M. Faulenbach, et al. (2007). "Interleukin-1-receptor antagonist in type 2 diabetes mellitus." N Engl J Med **356**(15): 1517-26.

Li, J. and J. Yuan (2008). "Caspases in apoptosis and beyond." Oncogene **27**(48): 6194-206.

Luthi, A. U. and S. J. Martin (2007). "The CASBAH: a searchable database of caspase substrates." Cell Death Differ **14**(4): 641-50.

Mahrus, S., J. C. Trinidad, et al. (2008). "Global Sequencing of Proteolytic Cleavage Sites in Apoptosis by Specific Labeling of Protein N Termini." Cell.

Mariathasan, S., D. S. Weiss, et al. (2006). "Cryopyrin activates the inflammasome in response to toxins and ATP." Nature **440**(7081): 228-32.

Martinon, F., V. Petrilli, et al. (2006). "Gout-associated uric acid crystals activate the NALP3 inflammasome." Nature **440**(7081): 237-41.

Martinon, F. and J. Tschopp (2005). "NLRs join TLRs as innate sensors of pathogens." Trends Immunol **26**(8): 447-54.

Miceli-Richard, C., S. Lesage, et al. (2001). "CARD15 mutations in Blau syndrome." Nat Genet **29**(1): 19-20.

Monod, J., J. Wyman, et al. (1965). "On the Nature of Allosteric Transitions: A Plausible Model." J Mol Biol **12**: 88-118.

O'Brien, T., B. T. Fahr, et al. (2005). "Structural analysis of caspase-1 inhibitors derived from Tethering." Acta Crystallogr Sect F Struct Biol Cryst Commun **61**(Pt 5): 451-8.

O'Neill, L. A. (2006). "How Toll-like receptors signal: what we know and what we don't know." Curr Opin Immunol **18**(1): 3-9.

O'Neill, L. A. (2008). "The interleukin-1 receptor/Toll-like receptor superfamily: 10 years of progress." Immunol Rev **226**: 10-8.

Ogura, Y., D. K. Bonen, et al. (2001). "A frameshift mutation in NOD2 associated with susceptibility to Crohn's disease." Nature **411**(6837): 603-6.

Petrilli, V., C. Dostert, et al. (2007). "The inflammasome: a danger sensing complex triggering innate immunity." Curr Opin Immunol **19**(6): 615-22.

Pop, C. and G. S. Salvesen (2009). "Human caspases: activation, specificity, and regulation." J Biol Chem **284**(33): 21777-81.

Riedl, S. J. and Y. Shi (2004). "Molecular mechanisms of caspase regulation during apoptosis." Nat Rev Mol Cell Biol **5**(11): 897-907.

Rothwell, N. (2003). "Interleukin-1 and neuronal injury: mechanisms, modification, and therapeutic potential." Brain Behav Immun **17**(3): 152-7.

Scheer, J. M., M. J. Romanowski, et al. (2006). "A common allosteric site and mechanism in caspases." Proc Natl Acad Sci U S A **103**(20): 7595-600.

Schmitz, J., A. Owyang, et al. (2005). "IL-33, an interleukin-1-like cytokine that signals via the IL-1 receptor-related protein ST2 and induces T helper type 2-associated cytokines." Immunity **23**(5): 479-90.

Schroder, K. and J. Tschopp (2010). "The inflammasomes." Cell **140**(6): 821-32.

Shi, Y. (2002). "Mechanisms of caspase activation and inhibition during apoptosis." Mol Cell **9**(3): 459-70.

Shi, Y., J. E. Evans, et al. (2003). "Molecular identification of a danger signal that alerts the immune system to dying cells." Nature **425**(6957): 516-21.

Swain, J. F. and L. M. Gierasch (2006). "The changing landscape of protein allostery." Curr Opin Struct Biol **16**(1): 102-8.

Taylor, R. C., S. P. Cullen, et al. (2008). "Apoptosis: controlled demolition at the cellular level." Nat Rev Mol Cell Biol **9**(3): 231-41.

Thornberry, N. A., H. G. Bull, et al. (1992). "A novel heterodimeric cysteine protease is required for interleukin-1 beta processing in monocytes." Nature **356**(6372): 768-74.

Timmer, J. C. and G. S. Salvesen (2007). "Caspase substrates." Cell Death Differ **14**(1): 66-72.

Walters, J., C. Pop, et al. (2009). "A constitutively active and uninhibitable caspase-3 zymogen efficiently induces apoptosis." Biochem J **424**(3): 335-45.

Chapter 2:

An allosteric circuit in caspase-1

2.1 Introduction

Allostery, functional coupling between sites on proteins, is central to biological regulation. This phenomenon has been classically examined in hemoglobin and in aspartate transcarbamoylase (ATCase), and generalized to many other regulatory enzymes involved in metabolic and signaling pathways, as well as in membrane and nuclear receptors (for recent review see (Changeux and Edelstein 2005)). While structural changes brought on by allostery are well documented the functional roles of amino acid side chains that couple conformational changes are less well understood. In this study, we begin to systematically examine the functional importance of amino acid side chains to couple conformational changes between sites in caspase-1.

Caspases are dimeric thiol proteases that drive cellular processes such as apoptosis and inflammation. These enzymes have at least two conformational states that are observed crystallographically and represent both active and inactive zymogen conformations (for review see (Fuentes-Prior and Salvesen 2004; Shi 2004)). The active conformation of caspase-1 has been crystallized with substrate mimics bound to the active site, and these represent the on-state conformation of the enzyme.(Romanowski, Scheer et al. 2004; Scheer, Romanowski et al. 2006) Recently, specific allosteric small molecule ligands have been captured at a cysteine residue at the dimer interface of apoptotic caspases-3 and -7 (Hardy, Lam et al. 2004), as well as the inflammatory caspase caspase-1 (Scheer, Romanowski et al. 2006). These ligands bind to a site ~15 Å from the active site and trap an inactive conformation of caspases. This off-state conformation is similar to the inactive zymogen form of caspase-7 (Hardy, Lam et al. 2004), or the ligand-free form of caspase-1 (Romanowski, Scheer et al. 2004), and therefore represents a natural state of these proteases (Figure 2.1).

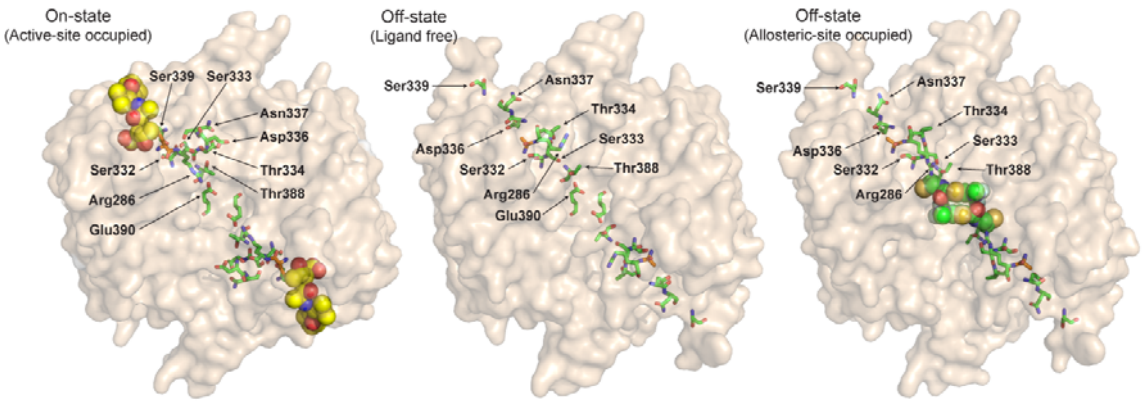

Figure 2.1. Conformational states of caspase-1. Locations of the residues involved in the hydrogen bonding network (highlighted in green sticks) of dimeric caspase-1 containing the active site inhibitor z-VAD-FMK (on-state, left; PDB ID code 2HBQ), or active-site ligand-free (off-state, middle; PDB ID code 1SC1), or containing an allosteric inhibitor (off-state, right; PDB ID code 2FQQ). The active-site Cys285 (C285A in off-state structures) is shown in orange and the inhibitors are shown in spheres. The Glu390 residue is hidden behind the allosteric inhibitor in the bottom structure.

Caspase-1 shows positive cooperativity indicating that binding of substrate at one active site enhances catalysis at the second site. Inspection of the X-ray structures for the active and allosterically inhibited enzyme suggests that coupling may be mediated by a network of 21 hydrogen bonding (H-bonding) interactions primarily involving 9 side chains (Figure 2.2). This network runs from one active site through the allosteric site to the second active site. Eight of the nine H-bonding residues in the network are completely conserved among the inflammatory caspases-1 and -5, and a close homolog caspase-4. (The Asp336 in caspase-1 is a histidine in caspases-4 and -5.) Overall, procaspase-1 has about 45% sequence identity with procaspases-4 and -5, which have 66% sequence identity with each other. One key interaction in caspase-1 appears to be a salt bridge between Arg286 and Glu390, as the allosteric inhibitors in caspase-1 directly disrupt this network by preventing the salt bridge from forming (Scheer, Romanowski et al. 2006).

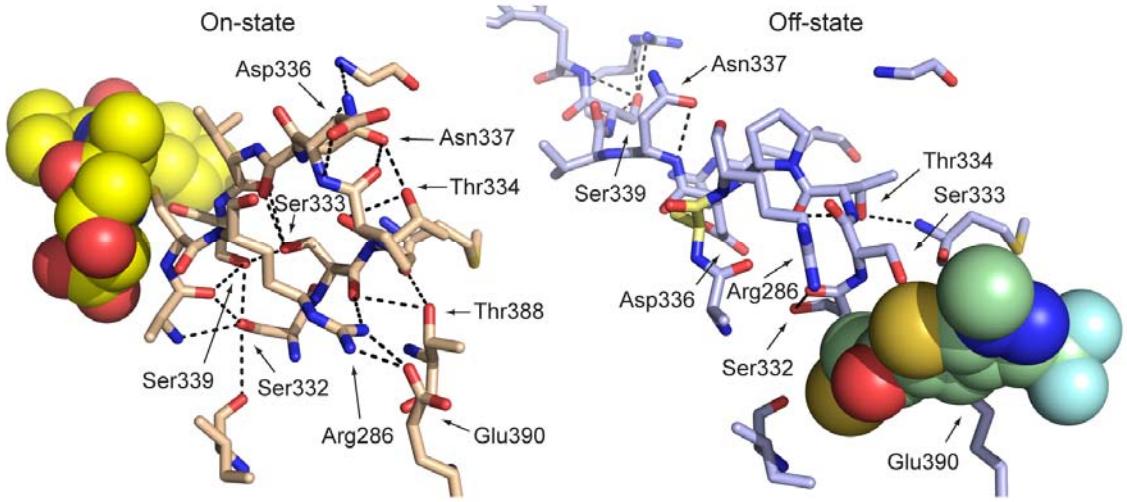

Figure 2.2. **Residues that form a hydrogen bonding network and a salt bridge that connects the active and the allosteric ligand sites of caspase-1.** In the on-state conformation (left), many H-bond interactions involving polar side chains are formed which are not preserved in the off-state conformation (right). Dashed lines indicate a distance of less than 3.5 Å between two polar atoms. Yellow spheres represent the z-VAD-FMK active site inhibitor in the on-state structure (PDB ID code 2HBQ); green spheres represent the allosteric inhibitor in the off-state structure (PDB ID code 2FQQ)(Scheer, Romanowski et al. 2006). The active site cysteine (Cys285) is replaced with alanine (orange) in the off-state structure, and Thr388 is hidden behind the allosteric inhibitor.

To better understand the importance of residues in the H-bonding network in caspase-1 for enzyme activity, we employed alanine–scanning mutagenesis. This approach has been effective for systematic identification of functional “hot-spots” in protein interfaces (Clackson and Wells 1995) (for recent review see (Moreira, Fernandes et al. 2007)). Here, alanine-scanning mutational analysis shows that only four of the nine side chains, including the salt bridge, are significantly important for enzyme activity. These form a contiguous circuit of residues, or “hot wire” that runs from one active site to the dimer interface and on to the allosteric site. Such allosteric circuits may be revealed by mutational analysis in other cooperative enzymes and help to identify important functional determinants for allosteric coupling and activity.

2.2 Mutational analysis of the hydrogen bonding network in caspase-1

Active forms of caspase-1 have been crystallized bound to the active site inhibitors Ac-WEHD-CHO (Rano, Timkey et al. 1997) and to z-VAD-FMK (Scheer, Romanowski et al. 2006) (Figure 2.1, left; PDB ID code 2HQB). It has also been crystallized as an active-site ligand-free enzyme (Romanowski, Scheer et al. 2004) (Figure 2.1b, middle; PDB ID code 1SC1), and in the allosterically inhibited form (Scheer, Romanowski et al. 2006) (Figure 2.1c, right; PDB ID code 2FQQ). The active-site ligand-free and allosterically inhibited conformations are nearly identical, suggesting that they represent a natural off-state of the protease. The on- and off-states appear to be in dynamic equilibrium. These states can be trapped in caspase-1 (Scheer, Romanowski et al. 2006) or caspase-7 (Hardy, Lam et al. 2004) with site-specific covalent inhibitors to either the active site or allosteric site. The labeling is mutually exclusive since for both enzymes, binding of an active-site inhibitor blocks binding of an allosteric inhibitor, and vice versa.

The on-state of caspase-1 shows a complex network of 21 protein-protein H-bonds that connects the active site to the allosteric site (Table 2.1). In contrast, only 12 H-bonds are present in the off-state, and of these, only one is preserved in the on-state. The 9 side chains that dominate these H-bonding interactions form a contiguous network between the active and allosteric sites including a central Arg286 to Glu390 salt bridge (Figure 2.2). We wished to probe how important this H-bonding network is to the activity of caspase-1. Thus, we systematically replaced with alanines the nine H-bonding residues whose side chain positions change significantly (>3-5 Å) when caspase-1 switches from the on- to off-state (Table 2.1). The variants were expressed, and purified, and kinetically analyzed as described in the Materials and Methods.

Table 2.1. Potential intramolecular hydrogen bonds formed by polar side chains. †

Side Chain	Active-site ligand-bound	Active-site ligand-free
Arg 286	Arg 286 Nη1 : Glu 390 Oε1 Arg 286 Nη1 : Ser 333 O Arg 286 Nη2 : Glu 390 Oε1	No intramolecular contacts
Ser 332	Ser 332 Oγ : Ser 339 Oγ Ser 332 Oγ : Ala 284 O Ser 332 Oγ : Ala 284 N Ser 332 Oγ : Ile 282 O	Ser 332 Oγ : Ser 332 O
Ser 333	Ser 333 Oγ : Ser 339 Oγ Ser 333 Oγ : Asn 337 O Ser 333 Oγ : Val 388 O	No intramolecular contacts
Thr 334	Thr 334 Oγ1 : Asn 337 Oδ1 Thr 334 Oγ1 : Thr 334 O	No intramolecular contacts
Asp 336	Asp 336 Oδ1 : Arg 240 Nη1 Asp 336 Oδ1 : Asp 336 N Asp 336 Oδ2 : Arg 240 Nη1	Asp 336 Oδ1 : Asp 336 O Asp 336 Oδ1 : Arg 383 Nη1 Asp 336 Oδ2 : Arg383 Nη1
Asn 337	*Asn 337 Oδ1 : Thr 334 Oγ1 Asn 337 Oδ1 : Pro 335 O Asn 337 Nδ2 : Asn 337 N Asn 337 Nδ2 : Gly 291 N	Asn 337 Oδ1 : Asn 337 N Asn 337 Nδ2 : Asn 337 O Asn 337 Nδ2 : Asn 337 N
Ser 339	*Ser 339 Oγ : Ser 333 Oγ *Ser 339 Oγ : Ser 332 Oγ Ser 339 Oγ : Ala 284 O	Ser 339 Oγ : Arg 341 O Ser 339 Oγ : Trp 340 N
Thr 388	Thr 388 Oγ1 : Ser 333 O Thr 388 Oγ1 : Met 386	Thr 388 Oγ1 : Glu 390 Oε1 Thr 388 Oγ1 : Thr 388 O
Glu 390	*Glu 390 Oε1 : Arg 286 Nη1 *Glu 390 Oε1 : Arg 286 Nη2	*Glu 390 Oε1 : Thr 388 Oγ1 Glu 390 Oε2 : Arg 391 N
Total # of unique H-bonds :	21	12

†Potential H-bonds based on PDB ID code 2HBQ for active-site ligand-bound structure and PDB ID code 1SC1 for active-site ligand-free structure.
*Indicates potential hydrogen bond listed earlier in this table under interacting partner.

In general, the effects of alanine substitution differed widely (Table 2.2). Five of the variants (S333A, T334A, D336A, N337A, and T388A) caused minor reductions in k_{cat}/K_M of 2-fold or less. In contrast, two variants caused moderate reductions in k_{cat}/K_M of about 4-fold (S332A) and 7-fold (S339A), and two caused large reductions of 230- and 130-fold (R286A and E390A, respectively). Generally, the effects showed up as a mixture of both increases in K_M, and decreases in the k_{cat}. For hydrolysis of amides, acylation is rate-limiting and thus K_M approximates the K_d for substrate binding (Gutfreund and Sturtevant 1956). Therefore much of these effects reflect reduced binding affinity of substrate, although for the S332A variant most of the effect appeared in k_{cat}.

It is useful to interpret these data in the context of the structure of the on- and off-states of caspase-1. Four of the H-bonding side chains, Ser332, Ser333, Ser339, and Thr388, form a cluster that lies behind loop 2 (residues 285-290), which contains the catalytic Cys285. This cluster appears to stabilize this region which forms the floor of the substrate-binding site in the on-state (Figure 2.2, left). In the ligand-free or allosteric ligand-bound conformations (off-states), these loops undergo a large conformational change, breaking almost all of these H-bonds (Figure 2.2, right). We determined the structure of the T388A variant in complex with the z-VAD-FMK active-site inhibitor. The Arg286 and Glu390 side chains involved in the salt bridge interaction adopted different rotamers in the T388A variant (PDB ID code 2H54), but the structure was otherwise virtually identical to the wild type enzyme (data not shown). The S332A and S339A substitutions, which are located most centrally in this cluster directly under the active site, cause larger reductions in k_{cat}/K_M compared to substitutions at the more peripherally located Ser333 and Thr388 positions.

Table 2.2. Kinetic data for alanine-scan mutants of the caspase-1 hydrogen-bonding network.

Construct	K_M, μM	k_{cat}, sec^{-1}	k_{cat}/K_M, $M^{-1}\bullet sec^{-1}$	Ratio† k_{cat}/K_M	n_{HILL}	H-bonds Active	H-bonds Apo
Wild type	12	0.65	5.3×10^4	1	1.4		
R286A	230	0.055	2.4×10^2	230	1.8	3	0
S332A	3.2	0.055	1.4×10^4	3.7	1.4	4	1
S333A	15	0.38	2.5×10^4	2.0	1.8	3	0
T334A	18	0.55	3.1×10^4	1.7	1.7	2	0
D336A	21	0.78	3.8×10^4	1.4	1.5	3	3
N337A	13	0.41	3.0×10^4	1.8	1.7	4	3
S339A	25	0.20	7.9×10^3	6.7	1.6	3	2
T388A	8.6	0.24	2.8×10^4	1.9	1.6	2	2
E390A	100	0.041	4.0×10^2	130	1.3	2	2
R286A/E390A	430	0.014	3.2×10^1	1700	1.6		

*Standard errors within 10% of reported values based on data collected in triplicate; †Ratio of k_{cat}/K_M relative to wild type.

Another part of the H-bonding network formed in the on-state of caspase-1 involves the side chains of Thr334, Asp336, and Asn337 (Figure 2.2, left). In the on-state conformation, these side chains make polar interactions that appear to stabilize loop 3 (residues 332 to 346). Loop 3 contains Arg341 and Trp340, which directly contacts the P1 and P2 substrate residues, respectively. In the off-state, Asp336 forms a new salt bridge with Arg383, but Thr334 makes no intramolecular H-bonds, and Asn337 only interacts with its backbone amide and carbonyl (Figure 2.2, right). Alanine substitutions at these three residues cause only minor reductions in k_{cat}/K_M within 2-fold. The dominant effect appears at the Arg286 to Glu390 salt bridge where alanine substitutions cause greater than 100-fold reductions in k_{cat}/K_M (Table 2.2). These effects are comparable to alanine substitutions in subtilisin that break direct H-bonds that stabilize the oxyanion transition state (Wells, Cunningham et al. 1986).

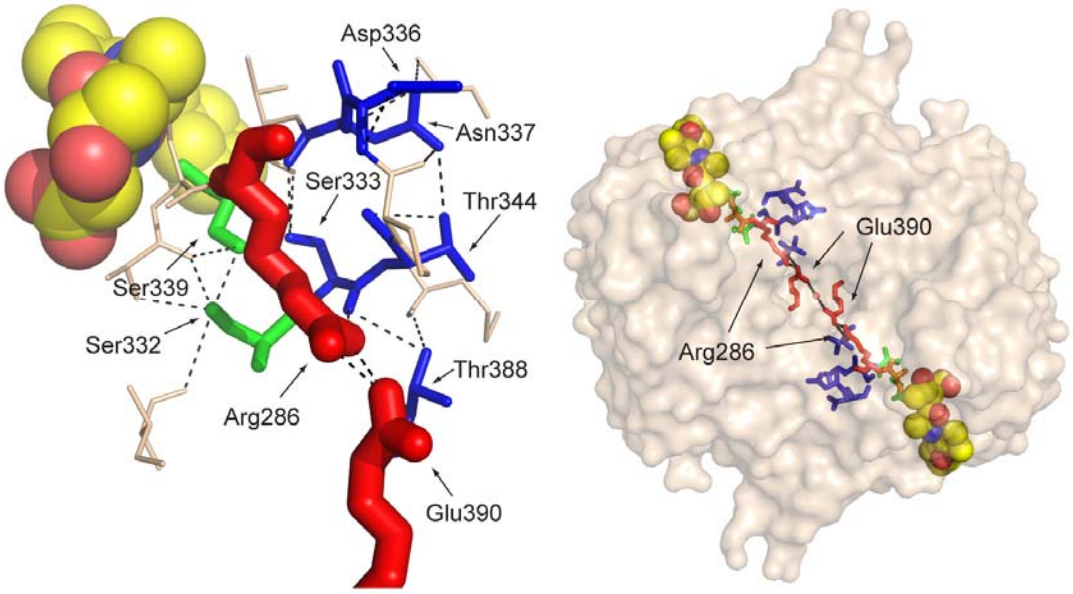

Figure 2.3. **Crucial residues for caspase-1 activity.** The left panel shows a size and color-coded representation of residues important for wild type caspase-1 activity. Larger residues had a larger impact when replaced with alanine; red, green, and blue indicate a >100-fold, >2-fold, and <2-fold decrease in k_{cat}/K_M relative to wild type. The allosteric site is located to the right of Glu390. The right panel shows an expanded view of the caspase-1 dimer. A circuit of residues connects the two active sites to the central allosteric site via the Arg286-Glu390 salt bridges. The yellow spheres represent the z-VAD-FMK active site inhibitor. This figure is derived from the active site bound on-state structure (PDB ID code 2HBQ).

The magnitude of these individual functional effects are not readily rationalized based on the change in H-bond inventory between the on- and off-states or the absolute number of H-bonds present in each state (Table 2.2). For example, some substitutions that break a net of three H-bonds when going from on- to off-state (R286A, S332A, S333A) cause reductions in k_{cat}/K_M ranging from 2 to 200-fold. A similar range (2 to 200-fold) is seen when the net change in H-bond inventory is zero or one (D336A, N337A, S339A, T388A, and E390A). Side chains seen engaged in many or few H-bonds in either state do not predict the effects of alanine substitution either. Thus, the extent of H-bonding or change in H-bonding is not a good predictor of its functional effect on the allosteric network. If one maps the magnitude of alanine substitution effects upon the side chains as they sit in the active conformation of caspase-1 one can see that

the most functionally critical side chains (Ser332, Ser339, Arg286 and Glu390) form a circuit that connects the active site and allosteric site (Figure 2.3, left). Viewing this circuit in the context of a dimeric protease, these residues effectively connect one active site to the central allosteric cavity and by symmetry to the second active site (Figure 2.3, right). We have found that caspase-1 shows positive cooperativity with a Hill coefficient, n_{Hill}, of ~1.4 (Table 2.2 and (Scheer, Romanowski et al. 2006)). Positive cooperativity indicates that binding at one active site enhances activity at the second active site. The values of (n_{Hill}) can range from 1-2 for a positive cooperative dimeric enzyme. The n_{Hill} value we find for caspase-1 is comparable to that of a classically positive cooperative enzyme such as glycogen phosphorylase (n_{Hill} =1.6; (Madsen and Shechosk.S 1967; Buchbinder, Guinovart et al. 1995)).

We determined the impact of alanine substitutions in the H-bonding network on the Hill coefficient. Interestingly, most mutations preserve or even enhance the n_{Hill} value indicating that binding of the substrate at one active site can still couple through to the other active site. Our data suggest that the cooperativity is a robust property in that it is not significantly impacted by single amino acid substitutions. The kinetic parameters reported here are nearly the same as those previously reported for wild type caspase-1 and the salt bridge mutants. However, the Hill coefficient for the E390A mutant was 1.0 in our previous work and is 1.3 here (Scheer, Romanowski et al. 2006). We believe this difference reflects the newer data being collected at a higher enzyme concentration and with more replicates.

2.3 Conservative substitutions of the Arg286/Glu390 salt bridge

To further dissect the importance of the central salt bridge for caspase-1 activity, we introduced less dramatic changes to the side chains by mutagenesis and determined their X-ray

structures. The Arg286 in the large subunit was replaced with a lysine (PDB ID code 2H4Y), and the Glu390 in the small subunit was replaced with an aspartate (PDB ID code 2H4W). We tested the effect of these substitutions individually and together on caspase-1 activity (Table 2.3). The conservative replacement of Arg286 with Lys caused the largest reduction, a 150-fold decrease in catalytic efficiency (k_{cat}/K_M). This decrease resulted from both lowering k_{cat} and raising K_M. In contrast, the conservative replacement of Glu390 with Asp caused only a 2-fold decrease in k_{cat}/K_M. Interestingly, the effect of the R286K/E390D variant (PDB ID code 2H51) was intermediate between the two single amino acid substitutions; the 37-fold decrease in activity of this variant relative to wild type suggests that the E390D substitution is able to partly restore catalytic function lost in the R286K variant. The effects on the n_{Hill} value were small as seen with the single-site alanine substitutions.

Table 2.3. Kinetic data for caspase-1 salt bridge variants.

Construct	K_M μM	k_{cat} sec^{-1}	k_{cat}/K_M, $M^{-1}\bullet sec^{-1}$	Ratio† k_{cat}/K_M	n_{HILL}
R286K	320	0.12	3.6×10^2	150	1.5
E390D	8.6	0.30	3.5×10^4	1.5	1.4
R286K/E390D	60	0.086	1.4×10^3	37	1.3

*Standard errors within 10% of reported values based on data collected in triplicate; †Ratio of k_{cat}/K_M relative to wild type (Table 2.2).

To better understand the effects of these substitutions on the active-form of caspase-1 we determined X-ray structures of the three enzyme variants labeled with the active-site inhibitor z-VAD-FMK to trap the active form of the enzyme and compared with active site labeled wild type caspase-1. The enzyme structures were determined at 1.8 Å to 2.1 Å resolution and refined with the covalent active-site inhibitor bound (Table 2.6, section 2.5.3). These showed that the overall structures of the variant enzymes were virtually identical to the wild type protein in the active conformation except for subtle changes in the key salt-bridge interaction (Figure 2.4). Interestingly, the R286K variant that showed the most drastic effect on catalytic activity, was the only variant to maintain the direct salt bridge of Lys286 to Glu390 (Figure 2.4a, b). In both the E390D variant and the R286K/E390D variant, a water-mediated salt bridge is formed (Figure 2.4c, d).

What could explain the lower activity of the R286K variant even when the salt bridge is maintained? In the wild type structure, solvent waters sit in the pocket behind Arg286, one of which is coordinated by the carbonyl of Arg240 and the γ-amine of Arg286 (Figure 2.4a). In the R286K variant, this water is only coordinated by the carbonyl of Arg240; the ε-amine of the lysine is held away from this pocket to form a salt bridge with Glu390 and is unable to coordinate solvent waters (Figure 2.4b). In contrast, the γ-amine of Arg286 in the E390D variant maintains coordination of water while the terminal amine forms an indirect salt bridge with the aspartate in the 390 position (Figure 2.4c). The indirect salt bridge is completed by a water molecule that sits between the γ-amine of Arg286 and the aspartate. In the R286K/E390D variant, the lysine and aspartate are too far separated to form a direct salt bridge. Instead, the ε-amine of lysine bends back toward the solvent pocket into a position where it is able to both coordinate a solvent water molecule and maintain an indirect salt bridge with the aspartate via a solvent water (Figure 2.4d). Thus, perhaps both stabilizing interactions with the solvent pocket

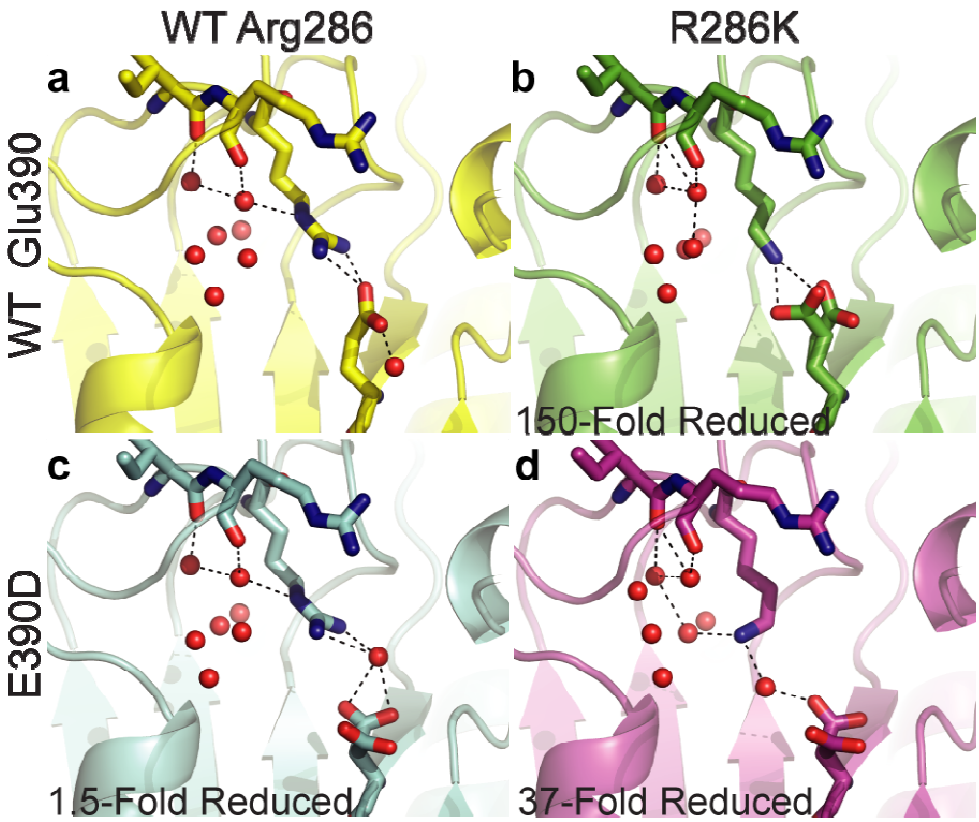

Figure 2.4. **Comparison of the salt bridge interaction in wild type caspase-1 and variants in the active conformation. (a)** The top left panel shows the configuration of the Arg286-Glu390 salt bridge in wild type caspase-1. The γ-amine of Arg286 coordinates a water molecule in the solvent pocket. **(b)** The top right panel shows the direct salt bridge formed between lysine at position 286 and Glu390; the ε-amine of the lysine does not coordinate solvent waters. **(c)** The bottom left panel shows the indirect salt bridge formed between Arg286 and the shortened acidic side chain of aspartate at position 390. **(d)** The bottom right panel shows the configuration of the indirect salt bridge formed in the R286K/E390D variant, which is able to restore activity lost in the R286K variant. The ε-amine of lysine bends back towards the solvent pocket to a position where it both coordinates a solvent water molecule and maintains an indirect salt bridge with the aspartate.

and maintaining a salt bridge interaction between the allosteric and active sites is important for preserving catalytic activity in caspase-1. It is also possible that these static structures of the on-state do not reveal the true stability of the on-form relative to the off-form. Although we see that the salt bridge can form in the R286K/E390D variant when trapped by binding the covalent active site inhibitor, the enzyme is clearly challenged to reach the active conformation.

2.4 Discussion

These mutational and structural studies begin to reveal the critical features of an extensive and conserved H-bonding network that couples the functional sites in caspase-1. The alanine-scanning experiments indicate that only four of the nine H-bonding side chains have a significant effect on activity, especially the Arg286-Glu390 interaction. These form a contiguous chain of interactions that connects the active and allosteric sites in the protease.

It is remarkable that so many of the H-bonding pairs seen in the on-state are not preserved in the off-state of caspase-1 (Table 2.1, Figure 2.2). From structural inspection alone it is difficult to predict which of the residues involved in this extensive H-bonding network are most critical for enzyme activity. Neither the extent of H-bonding in one state, nor the changes in H-bonding between on- and off-states predict which residues should be most important (Table 2.2). Including bound waters in the H-bond inventory still does not improve predictive power (Table 2.4). We conclude that changes in H-bonding patterns are not clear predictors of the effects on the activity we observe. In general the substitutions had fairly small effects on the Hill coefficient. Even the 130-230-fold reductions in activity seen for the E390D and R286A caused only slight changes in the Hill coefficient, suggesting the cooperativity is a fairly robust property of the enzyme.

The effects of conservative substitutions in the critical Arg286-Glu390 salt bridge on both the structure and function of the enzyme were somewhat surprising. One conservative shortening substitution (R286K) caused a 150-fold reduction in activity whereas another one (E390D) had only a small 2-fold reductions. This substitution combined with the R286K caused a partial restoration from the single R286K variant. The structures of the active forms of the

enzyme, driven by reaction with the active-site titrant z-VAD-FMK, did not provide an obvious structural interpretation for the functional effects. For example, we see that the direct salt bridge is preserved in the dramatically reduced R286K variant, but for the E390D variant a water-mediated salt bridge is seen between the Asp390 and Arg286. The most active variants are those that preserve both the salt bridge between positions 286 and 390 and the interaction with the water cluster. These latter interactions are lost in the R286K variant, and preserved in the more active R286K/E390D variant.

Solvent accessibility calculations (Table 2.5) show that Arg286 in the wild type structure is more solvent exposed than Lys286 in the mutant variant. This means that the new configuration in the R286K variant causes the salt bridge to be fully buried, and this could be energetically less favorable due to the internal environment of the protein not fully compensating for the desolvation of the salt bridge. We also calculated the solvent exposed polar and hydrophobic surface areas for the two salt bridge residues in each of the variants. Interestingly, we find that as exposed hydrophobic surface area increases and exposed polar surface area decreases, the activity of the variants also decreases. We are reluctant to make strong conclusions about the importance of specific H-bonding interactions with the water cluster based on this small data set. Nonetheless, we are impressed by the functional variation in these conservative substitutions.

Non-preserving effects for conservative substitutions of electrostatic interactions in other systems have also been reported. Studies of Ras have demonstrated that the Gln61 position is sensitive to mutations that can reduce the k_{cat} of the RasGAP complex by at least 1000-fold. Interestingly, computational studies found that despite the direct electrostatic interactions this residue makes with other residues and substrate in the transition state, it is not

Table 2.4. Potential hydrogen bonds formed by polar side chains, including solvent waters.[†]

Side Chain	Active-site ligand-bound	Active-site ligand-free
Arg 286	Arg 286 Nη1 : Glu 390 Oε1	Arg 286 Nη1 : H_2O
	Arg 286 Nη1 : Ser 333 O	
	Arg 286 Nη2 : Glu 390 Oε1	
	Arg 286 Nη2 : H_2O	
	Arg 286 Nε : H_2O	
Ser 332	Ser 332 Oγ : Ser 339 Oγ	Ser 332 Oγ : Ser 332 O
	Ser 332 Oγ : Ala 284 O	
	Ser 332 Oγ : Ala 284 N	
	Ser 332 Oγ : Ile 282 O	
	Ser 332 Oγ : H_2O	
Ser 333	Ser 333 Oγ : Ser 339 Oγ	No intramolecular contacts
	Ser 333 Oγ : Asn 337 O	
	Ser 333 Oγ : Val 338 O	
Thr 334	Thr 334 Oγ1 : Asn 337 Oδ1	No intramolecular contacts
	Thr 334 Oγ1 : Thr 334 O	
	Thr 334 Oγ1 : H_2O	
	Thr 334 Oγ1 : H_2O	
Asp 336	Asp 336 Oδ1 : Arg 240 Nη1	Asp 336 Oδ1 : Asp 336 O
	Asp 336 Oδ1 : Asp 336 N	Asp 336 Oδ1 : Arg 383 Nη1
		Asp 336 Oδ1 : H_2O
		Asp 336 Oδ1 : H_2O
	Asp 336 Oδ2 : Arg 240 Nη1	Asp 336 Oδ2 : Arg383 Nη1
	Asp 336 Oδ2 : H_2O	Asp 336 Oδ2 : H_2O
	Asp 336 Oδ2 : H_2O	
Asn 337	*Asn 337 Oδ1 : Thr 334 Oγ1	Asn 337 Oδ1 : Asn 337 N
	Asn 337 Oδ1 : Pro 335 O	Asn 337 Oδ1 : H_2O
	Asn 337 Oδ1 : H_2O	
	Asn 337 Nδ2 : Asn 337 N	Asn 337 Nδ2 : Asn 337 O
	Asn 337 Nδ2 : Gly 291 N	Asn 337 Nδ2 : Asn 337 N
	Asn 337 Nδ2 : H_2O	
Ser 339	*Ser 339 Oγ : Ser 333 Oγ	Ser 339 Oγ : Arg 341 O
	*Ser 339 Oγ : Ser 332 Oγ	Ser 339 Oγ : Trp 340 N
	Ser 339 Oγ : Ala 284 O	
Thr 388	Thr 388 Oγ1 : Ser 333 O	Thr 388 Oγ1 : Glu 390 Oε1
	Thr 388 Oγ1 : Met 386	Thr 388 Oγ1 : Thr 388 O
Glu 390	*Glu 390 Oε1 : Arg 286 Nη1	*Glu 390 Oε1 : Thr 388 Oγ1
	*Glu 390 Oε1 : Arg 286 Nη2	Glu 390 Oε1 : H_2O
	Glu 390 Oε1 : H_2O	Glu 390 Oε1 : H_2O
	Glu 390 Oε2 : H_2O	Glu 390 Oε2 : Arg 391 N
	Glu 390 Oε2 : H_2O	
Total # of unique H-bonds:	33	19

[†]Potential H-bonds based on PDB ID code 2HBQ for active-site ligand-bound structure and PDB ID code 1SC1 for active-site ligand-free structure.
*Indicates potential hydrogen bond listed earlier in this table under interacting partner.

Table 2.5. Solvent accessibility calculations for salt bridge residues.[†]

Table 2.5a. Total solvent exposed surface area for a single salt bridge at position 286 and 390 for caspase-1 variants (units in $Å^2$).

Construct	Total	Polar	Hydrophobic
Wild type	17.2	12.8	4.4
R286K	18.9	4.8	14.1
E390E	18.1	11.6	6.5
R286K/E390D	17.3	7.7	9.6

Table 2.5b. Solvent exposed surface area for individual atoms for side chain residues at position 286 and 390 for caspase-1 variants (units in $Å^2$, only atoms with accessible surface area are shown).

Wild type	R286K	E390D	R286K/E390D
Arg286	Lys286	Arg286	Lys286
Cγ – 2.7	Cγ – 2.2	Cγ – 2.9	Cγ – 2.6
Cδ – 0.0	Cδ – 0.0	Cδ – 0.2	Cδ – 1.3
Nε – 2.7	Cε – 7.6	Nε – 2.7	Cε – 0.4
Nη2 – 7.3	Nζ – 0.2	Nη2 – 8.9	Nζ – 5.6
Glu390	Glu390	Asp390	Asp390
Cβ – 0.7	Cβ – 0.8	Cβ – 2.4	Cβ – 4.1
Cγ – 0.0	Cγ – 0.3	Cγ – 1.0	Cγ – 1.2
Cδ – 1.0	Cδ – 3.4		
Oε2 – 2.8	Oε2 – 4.6	Oδ2 – 0.0	Oδ2 – 2.1

[†]These calculations were done using the WHATIF Web Interface based on the following structures: wild type – 2HBQ, R286K - 2H4Y, E390D – 2H4W, R286K/E390D – 2H51.

involved in a direct chemical way in GTP hydrolysis. Rather, this residue is crucial in helping to form the polar framework of the active site and mutations of Gln61 disrupt the preorganized environment necessary for catalysis (Shurki and Warshel 2004). The importance of electrostatic interactions has also been studied in the context of protein-protein interfaces. The structure of the p160 coactivator ACTR in complex with the ACTR-binding domain of CREB-binding protein, CBP, identified a buried Arg-Asp salt bridge in the midst of a binding interface largely dominated by hydrophobic residues (Demarest, Martinez-Yamout et al. 2002). Mutational studies of this salt bridge found that this interaction is especially important for specificity when discriminating between binding partners. Modification of this interaction by swapping the positions of the Arg and Asp residues to maintain the salt bridge abrogated binding (Demarest, Deechongkit et al. 2004). This observation is perhaps not surprising, as ion pairs reversal in stable local protein environments is generally destabilizing (Hwang and Warshel 1988). These environments tend to form prepolarized sites organized to stabilize an ion pair of a given polarity such that swapping the residues in a salt bridge, as in the case of the ACTR-CBP binding interaction, will be destabilizing even when an electrostatic interaction is preserved. We have made perturbations to the electrostatic interaction in caspases-1 that we expected to be less disruptive than those in these other systems, yet we were surprised to find a significant impact on the catalytic activity in the R286K variants. It is possible that the reduction in k_{cat}/K_m seen with a R286K substitution is caused by the disruption of a preorganized network of polar interactions essential for protease activity that involves not only the Arg286-Glu390 salt bridge, but also surrounding interactions involving solvent water molecules.

The classic model of allosteric transitions predicts that proteins can adopt alternate conformations that are present in a preexisting equilibrium even in the absence of regulatory ligands (Monod, Wyman et al. 1965). Recent studies in various systems have begun to provide

direct experimental evidence for this theory and have extended it to allosteric regulation involving covalent modifications in addition to ligand binding events. NMR relaxation experiments on the nitrogen regulatory protein C demonstrated that the activation of this protein by phosphorylation shifts a preexisting equilibrium between inactive and active conformations (Volkman, Lipson et al. 2001). In a similar vein, studies of the enzyme cyclophilin A found that the enzyme undergoes pre-sampling of conformational states in the absence of substrate that mimic the dynamics seen during catalysis. Specific mutations cause shifts in the relative populations between conformations. In addition, cyclosporin A, which binds and inhibits cyclophilin A, shifts the enzyme to a single state. Thus, this drug works by locking the isomerase in one conformation (Eisenmesser, Millet et al. 2005). It is known that disruption of a salt bridge between the catalytic (Asp236) and regulatory (Lys143) subunits in *Escherichia coli* aspartate transcarbamoylase (ATCase) disrupts cooperative binding of the aspartate substrate (Eisenstein, Markby et al. 1990; Newton and Kantrowitz 1990). More recent work using small-angle X-ray scattering has found that disruption of this salt bridge by substitution with alanine results in an enzyme variant that exists in a reversible equilibrium between at least two states in the absence of ligands (Fetler, Kantrowitz et al. 2007). This is in contrast to wild type ATCase, which exists predominantly in a low-activity, low-affinity state. Therefore, disruption of a salt bridge in ATCase destabilizes one state, allowing the protein to exist in an equilibrium between two states in solution. In the case of caspase-1, the apo form of the enzyme crystallizes in the same conformation as the allosterically-inhibited form. We believe that caspase-1, in solution, exists predominantly in an inactive conformation. The results presented here suggest that the active conformation, which is favored in the presence of an active-site ligand, is stabilized by the formation of the Arg286-Glu390 salt bridge. Disruption of this interaction could make it harder

for the enzyme to visit the active conformation, leading to the decreased activity of the salt-bridge variants.

Overall, our studies point to a small set of side chains that form a contiguous circuit connecting the active and allosteric sites as being the most important for activity in caspase-1. Bioinformatic approaches analyzing co-evolution of residues in large protein super families show patterns of conservation and co-variation suggestive of allosteric circuits. In these families, the majority of residues seem to evolve independently, while a small subset form a linked network that is positioned for long-range communication through the structure (Suel, Lockless et al. 2003). Mutational analysis at protein-protein interfaces reveal only a small subset of contact residues near the center of the binding interface drive the affinity of the interaction (Moreira, Fernandes et al. 2007). Our alanine-scanning data on caspase-1 support the view that allostery is transmitted predominantly by a small subset of connected residues.

2.5 Experimental Procedures

2.5.1 Caspase-1 Expression and Purification

Recombinant caspase-1 was prepared by expression in *Escherichia coli (E. coli)* as insoluble inclusion bodies followed by refolding (Romanowski, Scheer et al. 2004; Scheer, Wells et al. 2005). The p20 (residues 120 – 297) and p10 (residues 317 – 404) subunits of wild type human caspase-1 were cloned into NdeI and EcoRI restriction endonuclease sites of the pRSET plasmid (Invitrogen, Carlsbad, CA). Site-directed mutagenesis was performed using the QuikChange Site-Directed Mutagenesis Kit from Stratagene (La Jolla, CA).

Caspase-1 subunits were expressed separately in *E. coli* BL21(DE3) Star cells (Invitrogen). Cells were harvested following induction of a log phase culture with 1mM IPTG for 4 h at 37°C and then disrupted with a microfluidizer. The inclusion body pellets were isolated by centrifugation of lysate for 20 min at 4°C. Pellets were washed twice with 50 mM HEPES (pH 8.0), 300 mM NaCl, 1 M guanidine-HCl, 5 mM DTT, and 1% Triton X-100, and washed two more times with the same buffer without the detergent. The washed inclusion body pellets were solubilized in 6 M guanidine-HCl and 20 mM DTT, and stored frozen at -80°C.

Refolding of caspase-1 was done by combining guanidine-HCl-solubilized large and small subunits (10mg of large subunit and 20mg of small subunit) in a 250 mL beaker, followed by rapid dilution with 100 mL of 50 mM HEPES (pH 8.0), 100 mM NaCl, 10% sucrose, 1 M nondetergent sulfobetaine 201 (NDSB-201), and 10 mM DTT. Renaturation proceeded at room temperature for 6 h. Samples were centrifuged at 16,000 g for 10 minutes to remove precipitate, and then dialyzed overnight at 4°C against 50 mM sodium acetate (pH 5.9), 25 mM NaCl, 5% glycerol, and 4 mM DTT. Dialyzed protein was purified by cation exchange chromatography using a pre-packed 5 mL HiTrap SP HP column (GE Healthcare Bio-sciences Corp, Piscataway, NJ). Protein was eluted using a linear gradient of 0-1.0 M NaCl over 20 min in a buffer containing 50 mM sodium acetate (pH 5.9) and 5% glycerol. Peak fractions were pooled and β-ME was added to a concentration of 1mM before samples were stored frozen at -80°C.

2.5.2 Enzyme Kinetic Analysis

For kinetic analysis of caspase-1, protein was buffer exchanged using a NAP-5 Column (Amersham) into assay buffer containing 50 mM HEPES (pH 8.0), 50 mM KCl, 200 mM NaCl, 10 mM DTT, 0.1% 3-[(3-cholamidopropyl)dimethylammonio]-1-propanesulfonate (CHAPS). Protein

concentration was determined by active-site titration; (Stennicke and Salvesen 1999) caspase-1 was incubated in assay buffer with a titration from a zero to 2-fold stoichiometric ratio of active-site inhibitor z-VAD-FMK for 2 hrs at room temperature. The protein was diluted to an enzyme concentration of 50 nM and activity was determined using the fluorogenic substrate Ac-WEHD-AFC at 25 μM.(Rano, Timkey et al. 1997; Talanian, Quinlan et al. 1997; Thornberry, Rano et al. 1997)

Steady-state kinetic analysis was done by titrating enzyme with the Ac-WEHD-AFC substrate (typically from 200 μM to 0.25 μM, but up to 2mM for inactive variants). The enzyme concentration was set to 45 nM for all variants except those that showed large decreases in activity: 100 nM for the R286K, R286A, and E390A variants; and 500 nM for the R286A/E390A variant. Kinetic analysis performed at 15 nM gave the same n_{Hill} suggesting the cooperativity we observe is not dependent on the enzyme concentration (data not shown). Data was collected for 10 min using a Spectramax M5 microplate reader (Molecular Devices, Sunnyvale, CA) with excitation, emission, and cutoff filters set to 365 nm, 495 nm, and 435 nm, respectively.

Kinetic constants V_{max}, K_M, and the Hill coefficient (n_{Hill}) were calculated using GraphPad PRISM. The initial velocity (*v)*, measured in relative fluorescence units per unit time, was plotted versus the logarithm of substrate concentration. The model used to fit the data is a sigmoidal does-response curve with variable slope, and from this model all three kinetic constants were derived. The general equation of this model is Y = Bottom + (Top-Bottom)/(1+10^((LogEC_{50}-X)*HillSlope)), where Y is the initial velocity, X is the logarithm of the substrate concentration, and Top, Bottom, EC_{50} (K_M), and Hill Slope are free parameters fit to the data. A standard curve using pure AFC product was used to convert relative fluorescence units to units of concentration (μM). In determining kinetic constants for caspase-1 we observed that at saturating substrate

concentrations, the enzyme exhibited decreasing activity as substrate concentration increased, most likely due to substrate inhibition. In order to correctly fit our data using non-linear regression, data points exhibiting product inhibition were excluded.

2.5.3 Crystallization, Data Collection, and Structure Determination

Crystals of caspase-1 variants in complex with inhibitors were obtained by hanging-drop vapor diffusion at 4ºC against a reservoir of 0.1 M PIPES (pH 6.0), 200 mM Li_2SO_4, 25% PEG 2000 MME, 10 mM DTT, 3 mM NaN_3, and 2 mM $MgCl_2$ (Arg286Lys); 0.1 M PIPES pH (6.0), 350 mM $(NH_4)_2SO_4$, 20% PEG 2000 MME, 10 mM DTT, 3 mM NaN_3, and 2 mM $MgCl_2$ (Glu390Asp); 0.1 M PIPES (pH 6.0), 175 mM $(NH_4)_2SO_4$, 20% PEG 2000 MME, 10 mM DTT, 3 mM NaN_3, and 2 mM $MgCl_2$ (R286K/E390D). All crystals for data collection were cryoprotected in mother liquors supplemented with 20% (v/v) glycerol for 1-2 min and immersion in liquid nitrogen.

Table 2.6. Crystallographic data and refinement statistics.

Mutation	E390D	R286K	R286K E390D	T388A
PDB ID	2H4W	2H4Y	2H51	2H54
Space group	$P4_32_12$	$P4_32_12$	$P4_32_12$	$P4_32_12$
Cell constants	a=b=63.3 Å, c=161.3 Å	a=b=63.3 Å, c=141.6 Å	a=b=63.2 Å, c=141.5 Å	a=b=63.2 Å, c=162.1 Å
X-ray source	R-Axis IV	R-Axis IV	SSRL BL 1.5	R-Axis IV
Wavelength (Å)	1.54	1.54	1.16	1.54
Resolution (Å)	20-2.0	20-1.9	20-2.1	20-1.8
Number of observations	72514	65566	59667	215595
Number of reflections	22946	23520	17438	31401
Completeness (%)[a]	92.0 (98.9)	96.8 (90.6)	95.6 (82.7)	96.0 (89.3)
Mean $I/(\sigma I)$	6.6 (2.5)	6.1 (2.6)	8.8 (3.4)	8.8 (2.0)
R-merge on I[b]	0.057 (0.268)	0.065 (0.237)	0.049 (0.148)	0.042 (0.364)
Cutoff criteria	I<-3σ(I)	I<-3σ(I)	I<-3σ(I)	I<-3σ(I)
Model and refinement statistics				
Resolution range (Å)	20-2.0	20-1.9	20-2.1	20-1.8
Number of reflections[c]	19985 (1079)	19735 (1070)	15528 (834)	28552 (1522)
Completeness (%)	91.8	88.4	93.8	95.7
Cutoff criterion	|F|>0.0	|F|>0.0	|F|>0.0	|F|>0.0
Number of residues	256	250	254	258
Number of water molecules	179	189	215	271
R.m.s.d. bond lengths (Å)	0.006	0.006	0.008	0.006
R.m.s.d. bond angles (°)	0.888	0.879	1.001	1.287
Luzzatti error (Å)	0.263	0.243	0.246	0.246
Correlation factor[d]	0.927	0.925	0.921	0.935
R_{cryst}[e]	21.03	20.31	17.96	20.31
R_{free}	24.66	23.55	23.63	23.71
Ramachandran plot statistics[f]				
Most favored	200 (89.3%)	197 (89.5%)	204 (91.5%)	202 (89.4%)
Additional allowed	23 (10.3%)	22 (10.0%)	18 (8.1%)	23 (10.2%)
Generously allowed	1 (0.4%)	1 (0.5%)	1 (0.4%)	1 (0.4%)
Disallowed	0 (0.0%)	0 (0.0%)	0 (0.0%)	0 (0.0%)
Overall G-factor[g]	0.2	0.1	0.1	0.2

[a]Numbers in parenthesis indicate high-resolution shells: E390D: 2.07-2.0 Å; R286K: 1.97-1.9 Å; R286K/E390D: 2.17-2.1 Å; and T388A: 1.86-1.8 Å.

[b]$R_{merge} = \Sigma_{hkl}\Sigma_i|I(hkl)_i - \langle I(hkl)\rangle|/\Sigma_{hkl}\Sigma_i\langle I(hkl)_i\rangle$.

[c]Numbers in parentheses indicate the numbers of reflections used to calculate the R_{free} factor.

[d]Correlation factor between the structure factors and the model as calculated by SFCHECK (Vaguine, Richelle et al. 1999).

[e]$R_{cryst} = \Sigma_{hkl}|F_o(hkl) - F_c(hkl)|/\Sigma_{hkl}|F_o(hkl)|$, where F_o and F_c are observed and calculated structure factors, respectively.

[g]Computed with PROCHECK (Laskowski, MacArthur et al. 1993).

Diffraction data were collected under standard cryogenic conditions on Beamline 1-5 at the Stanford Synchrotron Research Laboratory using a *mar345* image plate detector (the Arg286Lys/Glu390Asp variant) or a Rigaku RU-3R rotating anode generator and an RAXIS-IV detector (remaining variants), processed and scaled with CrystalClear from Rigaku/Molecular Structure Corporation (Pflugrath 1999). The structures were determined from single-wavelength native diffraction experiments by molecular replacement with AMoRe (Navaza 2001) using a search model from a previously determined structure (PDB ID 1SC1). The refinement of the initial solutions with REFMAC (Murshudov, Vagin et al. 1997; Pannu, Murshudov et al. 1998; Murshudov, Vagin et al. 1999) yielded experimental electron density maps suitable for model building with O (Jones, Zou et al. 1991). The following residues were not visible in the electron density maps for the indicated protein-inhibitor complexes and were omitted from refinement of the final atomic models: 120-131, 146-148 and 317 (the R286K variant), 120-124 and 145-149 (the E390D variant), and 120-127, 146-148 and 317 (the R286K/E390D variant). PROCHECK (Laskowski, MacArthur et al. 1993) revealed no disallowed (φ, ψ) combinations and excellent stereochemistry (see Table 2.6 for a summary of X-ray data and refinement statistics).

2.5.4 Accession Numbers

The atomic coordinates and structure factors have been deposited in the Protein Data Bank (www.rcsb.org). The PDB ID codes of the structures presented in this work are 2H4W (E390D mutant), 2H4Y (R286K mutant), 2H51 (R286K/E390D mutant), and 2H54 (T388A mutant).

2.6 References

Buchbinder, J. L., J. J. Guinovart, et al. (1995). "Mutations in Paired Alpha-Helices at the Subunit Interface of Glycogen-Phosphorylase Alter Homotropic and Heterotropic Cooperativity." Biochemistry **34**(19): 6423-6432.

Changeux, J. P. and S. J. Edelstein (2005). "Allosteric mechanisms of signal transduction." Science **308**(5727): 1424-8.

Clackson, T. and J. A. Wells (1995). "A hot spot of binding energy in a hormone-receptor interface." Science **267**(5196): 383-6.

Demarest, S. J., S. Deechongkit, et al. (2004). "Packing, specificity, and mutability at the binding interface between the p160 coactivator and CREB-binding protein." Protein Sci **13**(1): 203-10.

Demarest, S. J., M. Martinez-Yamout, et al. (2002). "Mutual synergistic folding in recruitment of CBP/p300 by p160 nuclear receptor coactivators." Nature **415**(6871): 549-53.

Eisenmesser, E. Z., O. Millet, et al. (2005). "Intrinsic dynamics of an enzyme underlies catalysis." Nature **438**(7064): 117-21.

Eisenstein, E., D. W. Markby, et al. (1990). "Heterotropic effectors promote a global conformational change in aspartate transcarbamoylase." Biochemistry **29**(15): 3724-31.

Fetler, L., E. R. Kantrowitz, et al. (2007). "Direct observation in solution of a preexisting structural equilibrium for a mutant of the allosteric aspartate transcarbamoylase." Proc Natl Acad Sci U S A **104**(2): 495-500.

Fuentes-Prior, P. and G. S. Salvesen (2004). "The protein structures that shape caspase activity, specificity, activation and inhibition." Biochem J **384**(Pt 2): 201-32.

Gutfreund, H. and J. M. Sturtevant (1956). "The Mechanism of Chymotrypsin-Catalyzed Reactions." Proc Natl Acad Sci U S A **42**(10): 719-28.

Hardy, J. A., J. Lam, et al. (2004). "Discovery of an allosteric site in the caspases." Proc Natl Acad Sci U S A **101**(34): 12461-6.

Hwang, J. K. and A. Warshel (1988). "Why ion pair reversal by protein engineering is unlikely to succeed." Nature **334**(6179): 270-2.

Jones, T. A., J. Y. Zou, et al. (1991). "Improved methods for binding protein models in electron density maps and the location of errors in these models." Acta Crystallogr. A **47**(Pt 2): 110-9.

Laskowski, R. A., M. W. MacArthur, et al. (1993). "PROCHECK: a program to check the stereochemical quality of protein structures." J Appl Crystallogr **D26**: 283-91.

Laskowski, R. A., M. W. MacArthur, et al. (1993). "PROCHECK: a program to check the stereochemical quality of protein structures." J. Appl. Crystallogr. D **26**: 283-91.

Madsen, N. B. and Shechosk.S (1967). "Allosteric Properties of Phosphorylase B .2. Comparison with a Kinetic Model." Journal of Biological Chemistry **242**(14): 3301-&.

Monod, J., J. Wyman, et al. (1965). "On the Nature of Allosteric Transitions: A Plausible Model." J Mol Biol **12**: 88-118.

Moreira, I. S., P. A. Fernandes, et al. (2007). "Hot spots-A review of the protein-protein interface determinant amino-acid residues." Proteins **68**(4): 803-812.

Murshudov, G. N., A. A. Vagin, et al. (1997). "Refinement of macromolecular structures by the maximum-likelihood method." Acta Crystallogr. D **53**: 240-55.

Murshudov, G. N., A. A. Vagin, et al. (1999). "Efficient anisotropic refinement of macromolecular structures using FFT." Acta Crystallogr. D **55**: 247-55.

Navaza, J. (2001). "Implementation of molecular replacement in AMoRe." Acta Crystallogr. D **57**(Pt 10): 1367-72.

Newton, C. J. and E. R. Kantrowitz (1990). "The regulatory subunit of Escherichia coli aspartate carbamoyltransferase may influence homotropic cooperativity and heterotropic interactions by a direct interaction with the loop containing residues 230-245 of the catalytic chain." Proc Natl Acad Sci U S A **87**(6): 2309-13.

Pannu, N. S., G. N. Murshudov, et al. (1998). "Incorporation of prior phase information strengthens maximum-likelihood structure refinement." Acta Crystallogr. D **54**(Pt 6 Pt 2): 1285-94.

Pflugrath, J. W. (1999). "The finer things in X-ray diffraction data collection." Acta Crystallogr. D **55**: 1718-25.

Rano, T. A., T. Timkey, et al. (1997). "A combinatorial approach for determining protease specificities: application to interleukin-1beta converting enzyme (ICE)." Chem Biol **4**(2): 149-55.

Romanowski, M. J., J. M. Scheer, et al. (2004). "Crystal structures of a ligand-free and malonate-bound human caspase-1: implications for the mechanism of substrate binding." Structure **12**(8): 1361-71.

Scheer, J. M., M. J. Romanowski, et al. (2006). "A common allosteric site and mechanism in caspases." Proc Natl Acad Sci U S A **103**(20): 7595-600.

Scheer, J. M., J. A. Wells, et al. (2005). "Malonate-assisted purification of human caspases." Protein Expr Purif **41**(1): 148-53.

Shi, Y. (2004). "Caspase activation: revisiting the induced proximity model." Cell **117**(7): 855-8.

Shurki, A. and A. Warshel (2004). "Why does the Ras switch "break" by oncogenic mutations?" Proteins **55**(1): 1-10.

Stennicke, H. R. and G. S. Salvesen (1999). "Caspases: Preparation and characterization." Methods **17**(4): 313-319.

Suel, G. M., S. W. Lockless, et al. (2003). "Evolutionarily conserved networks of residues mediate allosteric communication in proteins." Nat Struct Biol **10**(1): 59-69.

Talanian, R. V., C. Quinlan, et al. (1997). "Substrate specificities of caspase family proteases." J Biol Chem **272**(15): 9677-82.

Thornberry, N. A., T. A. Rano, et al. (1997). "A combinatorial approach defines specificities of members of the caspase family and granzyme B. Functional relationships established for key mediators of apoptosis." J Biol Chem **272**(29): 17907-11.

Vaguine, A. A., J. Richelle, et al. (1999). "SFCHECK: a unified set of procedures for evaluating the quality of macromolecular structure-factor data and their agreement with the atomic model." Acta Crystallogr D **55**: 191-205.

Volkman, B. F., D. Lipson, et al. (2001). "Two-state allosteric behavior in a single-domain signaling protein." Science **291**(5512): 2429-33.

Wells, J. A., B. C. Cunningham, et al. (1986). "Importance of Hydrogen-Bond Formation in Stabilizing the Transition-State of Subtilisin." Philosophical Transactions of the Royal Society of London Series a-Mathematical Physical and Engineering Sciences **317**(1540): 415-423.

Chapter 3:

Conformational states in caspases

3.1 Introduction

Interleukin-1β-converting enzyme (ICE), or caspase-1, was the first protein of the caspase family to be identified and isolated in humans. It is the protease responsible for cleaving the pro-inflammatory cytokine interleukin-1β (IL-1β) to its active form (Cerretti, Kozlosky et al. 1992; Thornberry, Bull et al. 1992). IL-1β is an important mediator of the host response to infection through the innate immune system and a primary cytokine in inflammation (Martinon and Tschopp 2007). In the case of caspase-1, two zymogen pro-caspase-1 chains form a homodimer; cleavage and removal of the intrachain linker on each chain leads to the formation of large (p20) and small subunits (p10). The end result is that the active form of caspase-1 is a homodimer of two p20-p10 heterodimers (in total, a $(p20p10)_2$ tetramer).

In contrast to caspase-1, caspase-3 is not involved in the inflammatory response. Rather, it is an executioner caspase that is activated in cells in response to apoptotic stimuli where it goes on to cleave a variety of cellular targets ultimately leading to cell death. These proteases also differ in their substrate specificity; the optimal recognition motif for caspase-1 is the tetrapeptide WEHD, while caspase-3 prefers DEVD (Grutter 2000). Caspases-1 and -3 share only 25% sequence homology (compared to 45% homology between inflammatory caspases-1 and -5; and 49% homology between executioner caspases-3 and -7). Despite these differences, caspases-1 and -3 have the same general domain structure comprised of a large and small subunit generated by intrachain cleavage; this functional unit associates with another to form the active caspase homodimer (Grutter 2000).

The observation of positive cooperativity suggests that an enzyme is better at catalyzing substrate turn-over when both sites are occupied than when one site is occupied. The measured Hill coefficient of 1.4 for wild-type caspase-1 suggests a strong coupling between the two

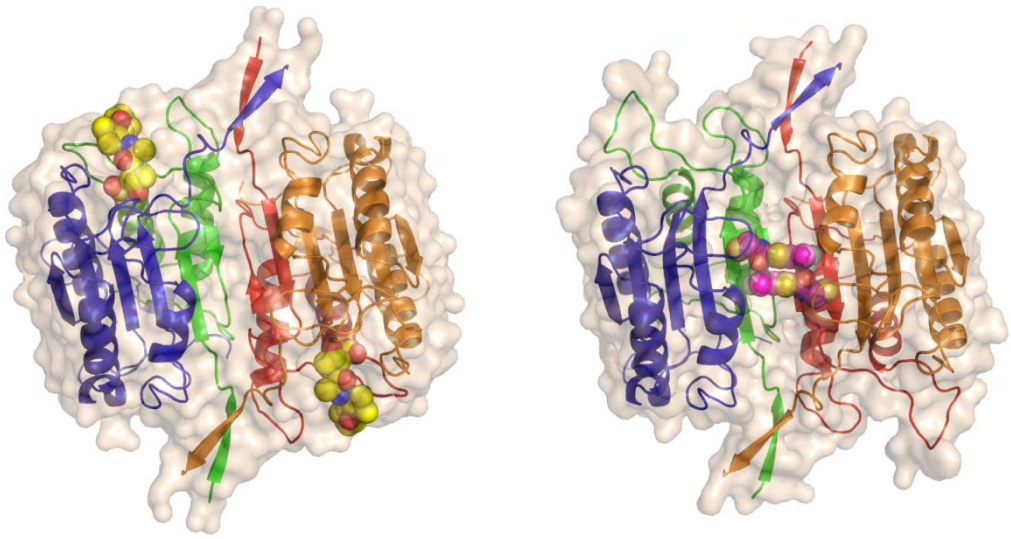

Figure 3.1. Conformational states of caspase-1. Structure of the caspase-1 dimer in the active conformation (left) bound to the active site inhibitor z-VAD-FMK (yellow spheres) and in the inactive conformation (right) bound to an allosteric inhibitor (purple spheres). The large subunits (p20) are colored blue and orange and the small subunits (p10) are colored green and red. As shown, the blue and green chains comprise the left half of the caspase-1 dimer, while the red and orange chains form the right half. The loops near the active sites (top left and bottom right of structures) undergo marked changes between conformations. This figure is based on PDB structures 2HQB and 2FQQ (Scheer, Romanowski et al. 2006).

catalytic sites (Datta, Scheer et al. 2008). Interestingly, caspase-1 is the only caspase that has been reported to demonstrate positive cooperativity. The Hill coefficient for executioner caspases (-3 and -7) is only 1.0-1.1, so these proteases do not act cooperatively.

What is the possible structural basis for the cooperativity seen in caspase-1? Various crystal structures of the enzyme suggest that cooperativity may be a result of a conformational change that occurs in the presence of substrate (Figure 3.1). When caspase-1 is crystallized in the presence of active site ligands, it adopts an active conformation characterized by the collapse of loop regions into a substrate binding pocket. On the other hand, when caspase-1 is crystallized with a ligand bound in an allosteric site or in the apo- form, it adopts an inactive conformation, with the active site loops open in a catalytically incompetent conformation

(Romanowski, Scheer et al. 2004; Scheer, Romanowski et al. 2006). In the case of caspase-3, the only crystal structures of the enzyme are in the active conformation when it is bound to active site inhibitors. However, caspase-3 is most closely related to caspase-7, which has been crystallized in the presence of both active site and allosteric site ligands and shows a similar conformational change as in caspase-1 (Hardy, Lam et al. 2004).

Based on the available enzymatic and structural data, we hypothesize that in the ligand-free state in solution, caspase-1 normally sits in an inactive conformation. The presence of substrate drives it to the active conformation, and this conformational switch, dependent on an increasing concentration of substrate, is measured as a Hill coefficient of 1.4. For caspase-3, we hypothesize that the enzyme is able to access active and inactive conformations as in the case of caspase-1 and -7, but the higher intrinsic activity of caspase-3 (as measured by k_{cat}/K_M) and lack of cooperativity suggests that this enzyme is already in the active conformation. The studies presented in this chapter seek to test these hypotheses through the use of chemical ligands and site-directed mutagenesis to probe the conformational states of caspases.

3.2 Activation of caspase-1 by sub-stoichiometric concentration of active-site inhibitor

Active-site titrations are a standard method used to determine the concentration of active enzyme in a given sample. The principle behind this assay involves titrating a known quantity of irreversible active-site inhibitor against a given protein concentration, and then measuring the enzyme activity. A plot of enzyme activity versus inhibitor to enzyme concentration ratio should give a linear decrease in the activity of the enzyme, and extrapolating this trend to complete enzyme inhibition gives an accurate measure of the inhibitor concentration needed to fully inhibit enzyme active sites, and thus a measure of the

concentration of enzyme active sites. The left-hand plot in Figure 3.2 shows a hypothetical active-site titration plot for a model enzyme.

In the case of caspases, the covalent, irreversible active-site inhibitor VAD-FMK can be used as an active-site titrant and is an effective inhibitor against all caspases (Stennicke and Salvesen 1999). Interestingly, active-site titrations performed against wild type caspase-1 do not show a linear decrease from baseline enzyme activity. Instead, sub-stoichiometric amounts of active-site inhibitor appear to increase the activity of the enzyme by as much as 50%, before complete labeling of active sites reduces enzyme activity to zero (Figure 3.2, right).

Why does the active-site titration plot for wild type caspase-1 vary so wildly from the plot for a model enzyme? In the case of our model enzyme, we assumed that the functional enzymatic unit contained only one active site. Thus, addition of an active-site inhibitor could only shut off the activity of a given enzyme molecule. However, the functional enzymatic unit of

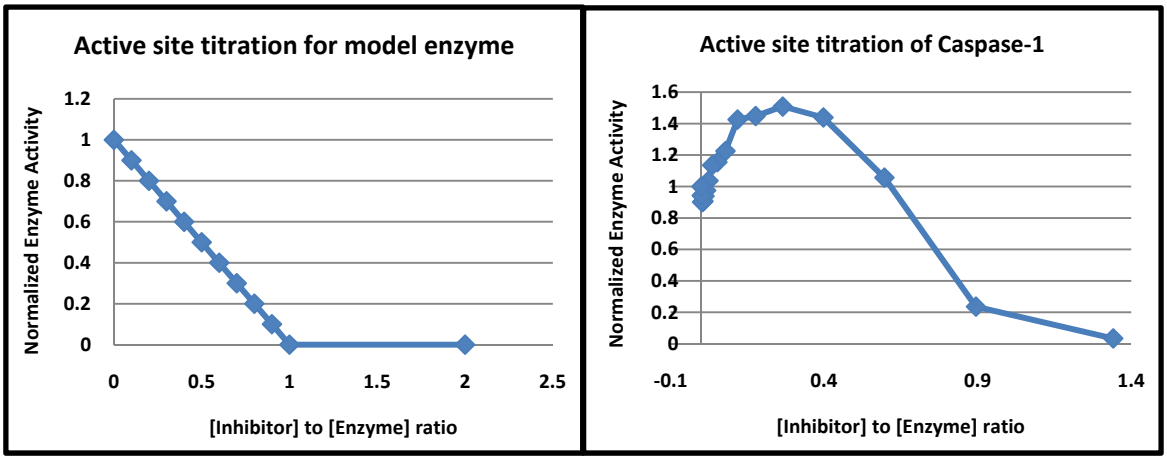

Figure 3.2. Active site titration of a model enzyme in comparison to caspase-1. The plot on left shows a hypothetical active-site titration for a model enzyme containing a single active site. As the inhibitor to enzyme concentration ratio increases from zero to one, the activity of the enzyme decreases linearly form baseline to zero. The right plot shows an active-site titration for caspase-1. Low inhibitor to enzyme concentration ratios activate the enzyme, suggesting the presence of a half-labeled caspase-1 species.

caspase-1 is a dimer, with two active sites. In this case, there is the possibility that a caspase-1 dimer will only have one active site occupied by the covalent inhibitor. Since caspase-1 with inhibitor in both active sites would have no activity, and caspase-1 with no inhibitor in either active site would have baseline activity, we can hypothesize that the activation we see in the caspase-1 active-site titration is due to the presence of "half-labeled" caspase-1 dimers.

Another possible explanation for the observation of activation with inhibitor is that the caspase-1 is in monomer-dimer equilibrium, with the activity of the monomer less than that of the dimer form. This sort of behavior has been noted previously for other proteases, notably in Kaposi's sarcoma associated herpesvirus (KSHV) protease (Pray, Reiling et al. 2002). The K_D for caspase-1 dimerization has been reported to be 30 nM (Talanian, Dang et al. 1996). Caspase-1 active-site titrations performed at a variety of enzyme concentrations above the K_D continue to show activation at low inhibitor to enzyme concentration ratios, suggesting that inhibitor-induced dimerization of caspase-1 is not solely the cause of the observed phenomenon.

Given the fact that wild type caspase-1 shows positive cooperativity, it is perhaps not surprising that caspase-1 behaves this way in the active-site titration. Though the Hill coefficient provides evidence for positive cooperativity in caspase, it only reports on the degree of subunit interaction, and its value does not go higher than the number of cooperative subunits (in this case two). It cannot provide information on the functional impact on the second active site after binding occurs in the first site. This raises the question as to what the activity of a single active site is when the other active site of the dimer is locked in the active conformation.

3.3 Expression and Preparation of half-labeled caspase constructs

To address this question, we developed a method for generating caspase "heterodimers" where only one active site of the caspase dimer is labeled with active-site inhibitor. Generating this construct allows us to examine what happens to the activity of one active site of a caspase dimer when the active site on the opposite dimer is locked in the active conformation through the use of a substrate mimic. X-ray crystal structures show that the conformation of caspase-1 is virtually identical whether the active site is occupied by various non-covalent or covalent inhibitors (Romanowski, Scheer et al. 2004). Therefore, it is possible to lock the enzyme in the active conformation by labeling with the irreversible active site inhibitor z-VAD-FMK. However, in order to generate this "half-labeled hybrid" construct, we must selectively label one subunit of the dimer while leaving the identical site on the other subunit unaffected.

We accomplished this in caspase-1 by first creating two affinity-tagged large subunits (p20), one with a His_6-affinity tag and the other with a Strep-affinity tag. In order to generate active caspase, we expressed the large and small subunits separately in *E. coli* where they form inclusion body pellets. Following purification of the subunits from pellets, affinity-tagged p20 subunits were refolded separately with wild-type p10 small subunit and then purified by cation exchange chromatography to generate the active caspase dimer. The pure His_6-tagged or Strep-tagged protein exhibited catalytic activity similar to wild-type caspase-1.

A schematic for generating half-labeled constructs of caspase is shown in Figure 3.3. The His_6-tagged caspase-1 construct was labeled with the irreversible active site inhibitor z-VAD-FMK to lock the active form of the enzyme, and then purified by gel filtration to remove excess inhibitor. This resulted in labeling of both active sites in the His_6-tagged homodimers as verified

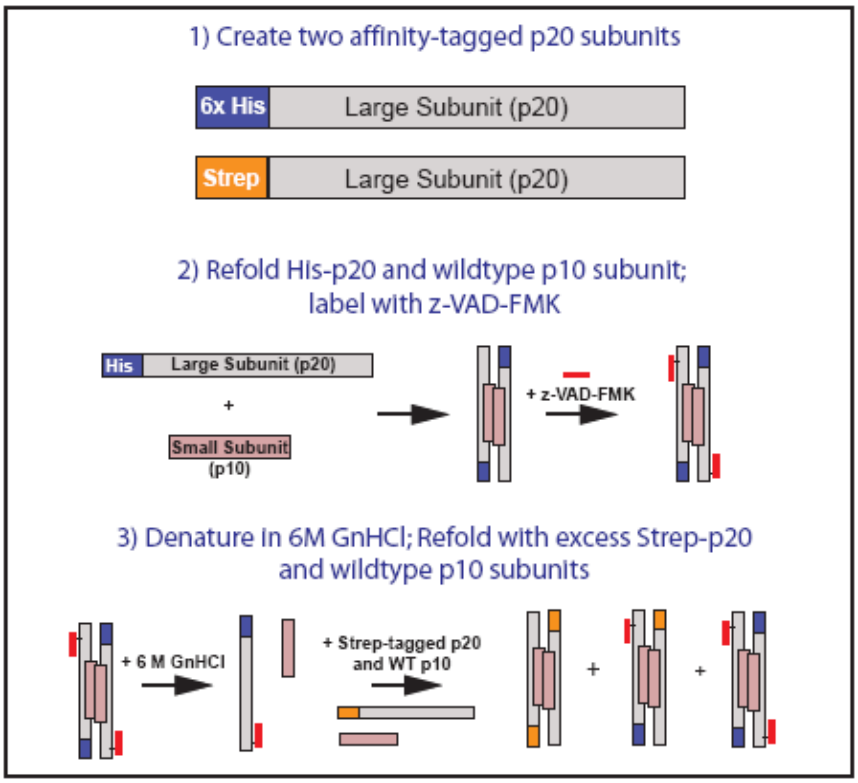

Figure 3.3. Schematic for expression of half-labeled caspase constructs. Generation of a half-labeled hybrid caspase-1 heterodimer involves complete labeling of a His_6-affinity tagged caspase-1 homodimer, followed by denaturation and refolding in the presence of a Strep-affinity tagged p20 subunit and additional p10 subunit.

by mass spectrometry and complete inhibition of catalytic activity. The labeled His_6-tagged caspase-1 was then denatured in 6M guanidine and refolded in the presence of the Strep-tagged p20 subunit and excess p10 subunit. This resulted in the generation of three caspase-1 species: (1) an unlabeled Strep-tagged protein; (2) a singly- or half-labeled His_6/Strep-tagged hybrid (3) and a doubly-labeled His_6-tagged protein. These three species could then be resolved by using sequential chromatography using the His_6- and Strep-affinity tags. Following size-exclusion chromatography to buffer exchange the enzyme and remove contaminants carried through the purification procedure, the purity of the heterodimeric half-labeled hybrid caspase-1 was verified by liquid chromatography-mass spectrometry.

3.4 Half-labeling of caspase-1 leads to activation of the protease

The impact on enzymatic activity of locking one active site of the caspase-1 dimer in the active conformation (half-labeled hybrid) was compared to the control (caspase-1 heterodimer containing both His_6- and Strep-affinity tags but no VAD-FMK labeling) by kinetic analysis. The labeled hybrid construct showed about a 10-fold increase in catalytic efficiency (per active subunit) that was due to a 20-fold increase in k_{cat} and a 2-fold increase in K_M (Table 3.1).

As would be expected, enzymatic assays showed that the half-labeled hybrid caspase-1 now behaved as a heterodimer with only one available active site. The Hill coefficient for the half-labeled hybrid was 1.1, reflecting the presence of a single active site, or at least decoupling of one active site from another. More conclusively, active-site titration of the half-labeled hybrid now showed a linear decrease in enzyme activity, as opposed to activation at low inhibitor to enzyme ratios (Figure 3.4). This data demonstrates that forcing one active site of the caspase-1 dimer into the active conformation greatly enhances the activity of the other active site, reinforcing the notion that the catalytic mechanism of this protease is highly cooperative.

Table 3.1. Half-labeling of the caspase-1 dimer leads to enzyme activation.

Construct	K_M μM	k_{cat} sec^{-1}	k_{cat}/K_M, $M^{-1}\bullet sec^{-1}$	Ratio k_{cat}/K_M
Unlabeled hybrid caspase-1	1.9	0.11	5.6×10^4	1
Half-labeled hybrid caspase-1	3.8	1.93	5.1×10^5	9.1

*Standard errors within 10% of reported values based on data collected in triplicate.

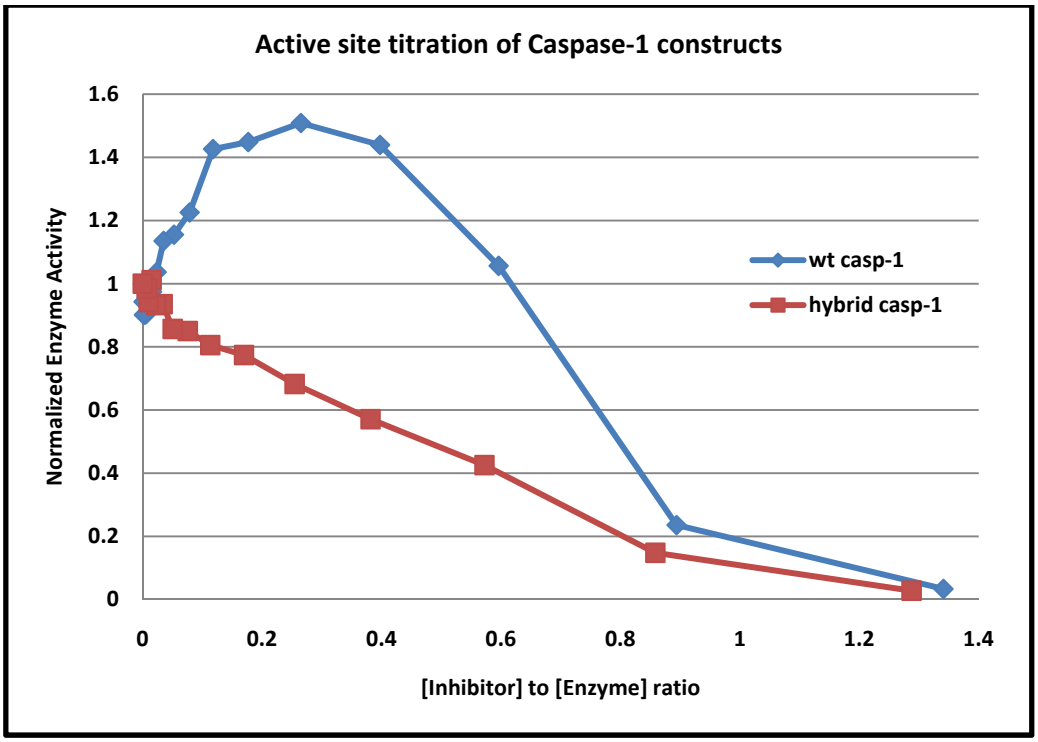

Figure 3.4. Active site titration of half-labeled hybrid caspase-1. The half-labeled caspase-1 heterodimer does not show activation at low inhibitor to enzyme concentration ratios as expected for an enzyme with a single active site.

3.5 Caspase-1 shows a greater degree of activation than caspase-3 as a result of half-labeling

As described previously, the executioner caspases, such as caspase-3, do not demonstrate positive cooperativity, suggesting that caspase-3 may already reside in a predominantly active conformation in contrast to caspase-1. To test this hypothesis, we decided to generate the corresponding caspase-3 heterodimer constructs using the methodology described above for caspase-1. The enzymatic activity of the half-labeled hybrid caspase-3 heterodimer was then compared to unlabeled caspase-3 heterodimer containing both affinity tags. As shown in Table 3.2, half-labeling of caspase-3 results in only a very slight increase in activity, if any. The activation is less than 2-fold in catalytic efficiency (k_{cat}/K_M), a result of an

increase in k_{cat} of about 2.5-fold and an increase in K_M of just over 2-fold. This is in stark contrast to the almost order of magnitude increase in caspase-1 catalytic efficiency due to half-labeling of the active sites.

Active-site titrations were performed on the caspase-3 heterodimer constructs in order to accurately determine enzyme concentration for the above enzyme kinetic assays. These plots show a steady linear decrease of enzyme activity from baseline as the inhibitor to enzyme ratio is increased (Figure 3.5). Taken together, these data support the notion that in contrast to caspase-1, an inflammatory caspase, the executioner caspase caspase-3 resides in the active conformation. The caspase-3 dimer is not activated when one active site is occupied by a substrate mimic.

Table 3.2. Half-labeling of the caspase-3 dimer results in minor enzyme activation.

Construct	K_M μM	k_{cat} sec^{-1}	k_{cat}/K_M, $M^{-1}\bullet sec^{-1}$	Ratio k_{cat}/K_M
Unlabeled hybrid caspase-3	13	1.4	1.1×10^5	1
Half-labeled hybrid caspase-3	28	3.7	1.3×10^5	1.3

*Standard errors within 10% of reported values based on data collected in triplicate.

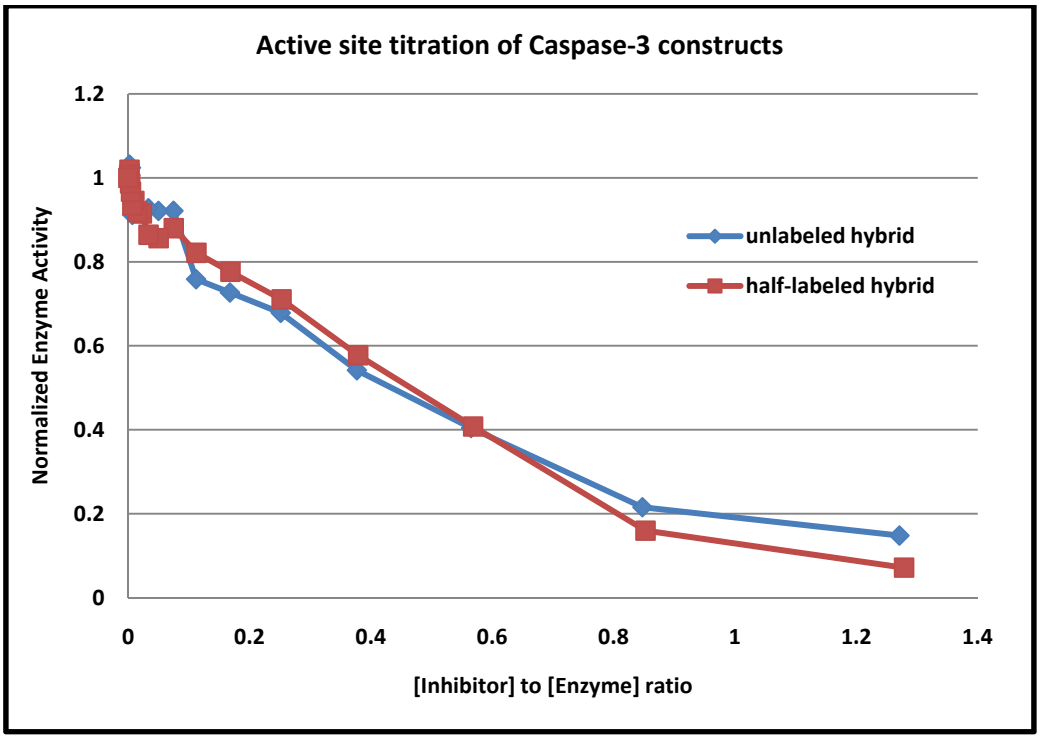

Figure 3.5. Active site titration of caspase-3 constructs. Caspase-3 constructs do not show activation at low inhibitor to enzyme concentration ratios, suggesting caspase-3 is in a predominantly active conformation.

3.6 Single residue mutants in caspase-1 select for conformational states

In the previous chapter, we reported on the presence of an extensive hydrogen-bonding network in the active conformation of caspase-1 that exists between the active and allosteric sites. This network is disrupted upon binding of the disulfide-trapped compounds in the allosteric site leading to large conformational changes that occur between the active and inactive conformations of caspase-1.

The glycine at position 287 in caspase-1 is located in the middle of the hydrogen-bonding network, and it appears to play a major role in allowing the conformational transition from the inactive to active state (Figure 3.6). As described in the previous chapter, the crystal

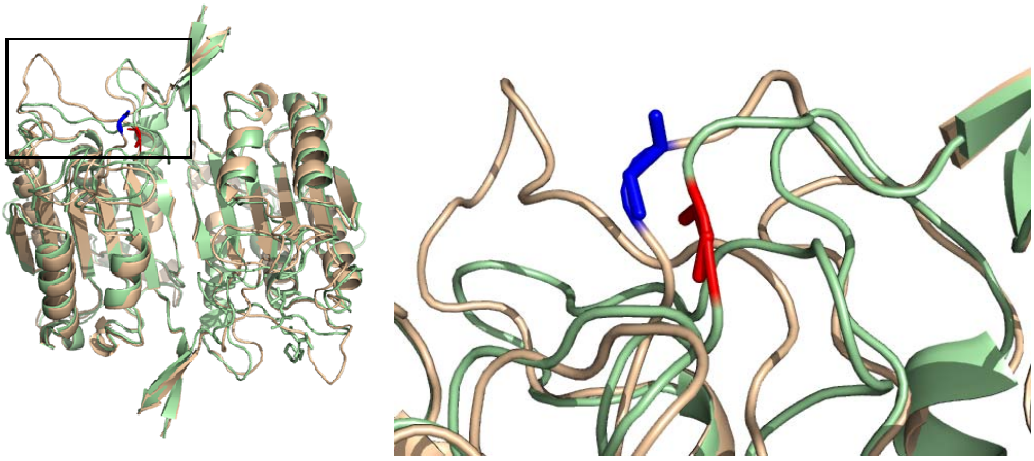

Figure 3.6. Glycine 287 is located in the middle of loop 2 and undergoes structural rearrangement from the inactive to active conformation. Comparison of caspase-1 structures with an active-site ligand (green) or ligand-free (beige) shows the movement of loop 2 as the enzyme goes from the inactive (ligand-free) to active conformation. The glycine at position 287 is highlighted blue in the inactive conformation and red in the active conformation.

structures of ligand-free and allosterically-inhibited caspase-1 show that these structures are nearly identical. Analysis of crystal structures of the active-site liganded and ligand-free conformations of caspase-1 demonstrate that Gly287 twists a net of 130° and 126° in ϕ and ψ angles, respectively, between the two conformations (Table 3.3). This allows loop 2 of the large subunit, which contains the active site cysteine at position 285 and the salt-bridge arginine at position 286, to rotate in and out of the active site. We decided to use site-directed mutagenesis to convert this glycine to an alanine and determine the importance of a glycine at this position.

Table 3.3. Dihedral angles for glycine 287 in active and apo structures.

Structure	Φ	ψ
Ligand-Free	149.4°	-174.3°
Active-site Ligand	-80.2°	59.5°

Table 3.4. Enzyme kinetic data for caspase-1 variants G287A and P343A.

Construct	k_{cat}/K_M, $M^{-1}\bullet sec^{-1}$	Ratio k_{cat}/K_M
Wild type caspase-1	5.3×10^4	1
G287A	3.5×10^1	1500
P343A	1.1×10^5	0.48

*Standard errors within 10% of reported values based on data collected in triplicate.

Our enzyme kinetic assays demonstrate that the G287A mutation causes a massive 1500-fold reduction in catalytic efficiency (Table 3.4). This is the largest decrease in caspase-1 activity that we have found for a single site mutation to alanine. In order to explain this observation, we mapped the dihedral angles of Gly287 shown in Table 3.3 onto a Ramachandran plot that shows the distribution of favored dihedral angles for alanine from structures in the Protein Data Bank. As shown in Figure 3.7, glycine adopts ϕ and ψ angles that are favorable for alanine in the ligand-free or inactive conformation, but it adopts ϕ and ψ angles that are forbidden for alanine in the active conformation. Therefore, we propose that the large reduction in caspase-1 activity that we see with the G287A variant is due to the presence of the alanine side chain locking the enzyme in an inactive conformation, since the alanine side chain is not compatible with the ϕ and ψ angles seen in the active conformation of caspase-1.

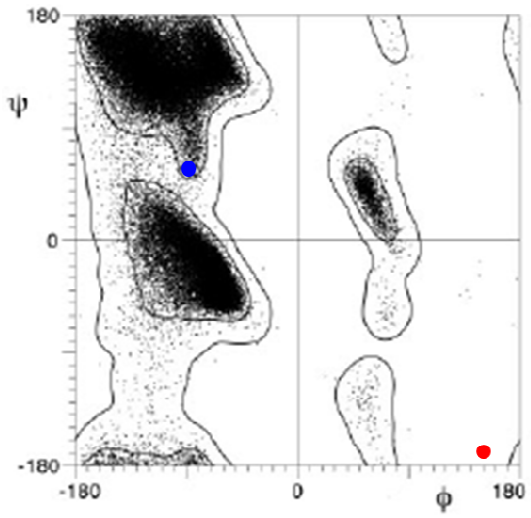

Figure 3.7. Ramachandran plot showing position of glycine 287 in caspase-1 active and apo structures. Mapping of the dihedral angles of glycine 287 from active and apo caspase-1 structures onto a Ramachandran plot (2HBQ and 1SC1, (Romanowski, Scheer et al. 2004) and (Scheer, Romanowski et al. 2006)). The Ramachandran plot for alanine is reproduced from (Lovell, Davis et al. 2003). Glycine adopts dihedral angles in the apo structure (inactive conformation) that are allowed for alanine (blue marker), but in the active structure (active conformation) those dihedral angle for alanine are prohibited (red marker).

The proline at position 343 in caspase-1 also appears to be intimately involved in the transition from the inactive to active conformation in caspase-1. This proline is located towards the C-terminal end of loop 3 of the small subunit, which contains many of the residues involved in the hydrogen bonding network and folds down in the active conformation to form the base of the substrate binding site. We used site-directed mutagenesis to convert Pro343 to an alanine and tested the effects using our enzyme kinetics assay. Surprisingly, we found that the P343A variant actually caused a 2-fold increase in caspase-1 catalytic efficiency (Table 3.4). Of all the caspase-1 variants we have made, this is the only alanine mutation that appears to confer an increase in activity to the enzyme. Because of their conformational rigidity in contrast to other amino acids, prolines are often found in turns. Based on the kinetic data and the positions of loop 3 found in the active and apo-structures of caspase-1 (Figure 3.8), we hypothesize that Pro343 stabilizes the folding of loop 3 to form the base of the active site in the active

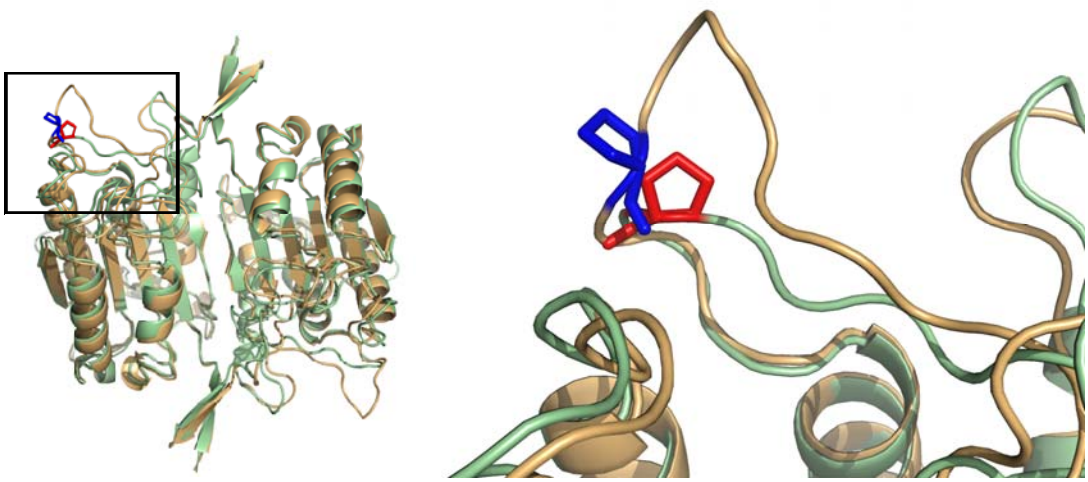

Figure 3.8. Proline 343 is located towards the C-teminal end of loop 3 and undergoes structural rearrangement from the inactive to active conformation. Comparison of caspase-1 structures with an active-site ligand (green) or ligand-free (beige) shows the movement of loop 3 as the enzyme goes from the inactive (ligand-free) to active conformation. The proline at position 343 is highlighted blue in the inactive conformation and red in the active conformation.

conformation, but that it also acts as a barrier to the conformational change from the inactive to active conformation. Introducing an alanine at this position relieves the rigidity in this turn, perhaps destabilizing the active conformation but making the transition more favorable and the caspase-1 dimer more likely to sample the active conformation, and this is measured as an increase in enzyme activity.

3.7 Binding of conformation-specific antibodies to caspase-1 variants

Given the large conformational change in caspase-1 when the active site is occupied versus not, our group proposed that it is possible to generate conformationally-selective antibody fragments (Fabs) to both the active state ("on-state") and allosterically inhibited state ("off-state") of the protein. Antibodies directed to specific conformational states have been

obtained by classical immunizations and monoclonal antibody methods (Li, Haruta et al. 2002; Jiang, Wang et al. 2004). Generally, the intrinsic conformational dynamics of proteins make it difficult to "trap" a single conformer and direct antibody selection to the desired conformation. However, in this case, active-site and allosteric-site inhibitors were used to trap mimics of the on- or off-states respectively as homogeneous antigens, and then raise antibodies corresponding specifically to the two states. Competitive ELISA shows that the binding of the on-state Fab is about 400-fold tighter to the on-state versus off-state of caspase-1, while the off-state Fab binds about 20-fold tighter to the off-state than the on-state, as measured by the K_D for binding using a surface plasmon resonance assay (SPR). Interestingly, the on-state Fab also enhances the activity of wild type enzyme about 3-fold compared to a non-cognate Fab made against VEGF (Gao, Sidhu et al. 2009). These Fabs provide us with a unique tool to test the conformation of caspase-1 in solution by measuring the binding properties of the Fabs against the enzyme.

In order to test our hypothesis that the G287A and P343A variants perturb the conformational state of caspase-1, we used our SPR assay to test the binding of the Fabs against these constructs. Our preliminary data shows that the on-state Fab has a slightly lower K_D for binding to P343A versus wild type enzyme, while the off-state Fab shows an almost order of magnitude reduction in K_D for binding to G287A than wild type enzyme (Table 3.5). Interestingly, the reduction in K_D indicating tighter binding of the Fabs appears to be due predominantly to changes in the k_{on} for the Fab binding to immobilized caspase-1. This would support our notion that alanine mutants have shifted the pre-existing conformational equilibrium of the caspase-1 dimer, making it easier for the conformation-specific Fab to bind to the molecule. These results are entirely consistent with the model that apo-caspase-1 is in a dynamic equilibrium between

Table 3.5. Binding of conformation-specific Fabs to G287A and P343 variants demonstrates shifts in caspase-1 conformation.

	Wild type K_D (10^{-9} M)	G287A K_D (10^{-9} M)	P343A K_D (10^{-9} M)
On-state Fab	330	N.D.	< 330
Off-state Fab	17	<< 17	N.D.

conformations, and that the G287A and P343A mutations perturb enzyme activity by driving caspase-1 into specific conformational states.

3.8 Discussion

In the previous chapter, we presented mutational and structural studies of caspase-1 that uncovered a linear circuit of functional residues running between the two active sites through the allosteric site. Enzymatic activity is strongly affected by perturbations of this circuit, suggesting that the interactions are important for stabilizing the active conformation of caspase-1. Kinetic analysis also demonstrated robust positive cooperativity, which is unique among caspases (Datta, Scheer et al. 2008). In this chapter, we have presented our work that uses both site-directed mutagenesis and chemical ligands to probe the conformational state of caspases.

As prototypical members of the inflammatory and executioner caspase families, caspase-1 and caspase-3 provide an interesting contrast in enzymatic properties. Previous work had demonstrated that while caspase-1 demonstrated positive cooperativity, caspase-3 did not. In addition, a comparison of baseline enzymatic activity of wild type enzyme shows that

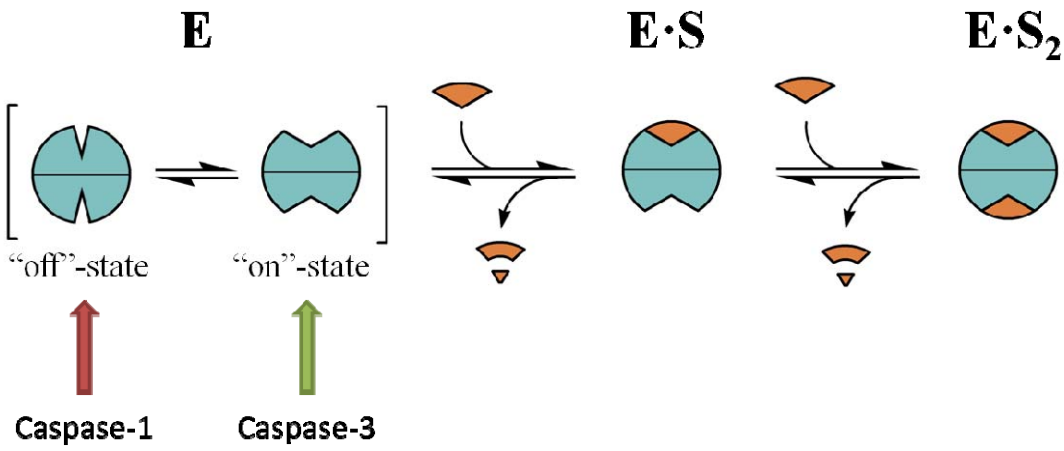

Figure 3.9. Model of caspase conformational states. Caspases exist in a conformational equilibrium between active and inactive states. The inflammatory caspase, caspase-1, resides primarily in the inactive conformation, and binding in the active site selects for the active conformation. The executioner caspase, caspase-3, resides primarily in the active conformation; binding in the active site has little additional effect on this equilibrium and enzyme activity.

caspase-3 is a more active protease than caspase-1 (almost an order of magnitude greater catalytic turnover, as measured by k_{cat}). We have now demonstrated that caspase-1 can be strongly activated by using the "half-labeling" technique to generate a hybrid caspase-1 heterodimer, whereas caspase-3 shows only a slight degree of activation in the same setting.

Taken together, these data suggest a model of caspase conformational states shown in Figure 3.9. The free caspase homodimer is in equilibrium between an inactive and active conformation. The observations of lower intrinsic catalytic turnover, positive cooperativity, and hybrid activation all point to caspase-1 residing primarily in the inactive conformation. In contrast, the higher intrinsic activity of caspase-3, lack of positive cooperativity, and inability to be activated by half-labeling all suggest that caspase-3 is sitting in a predominantly active conformation even in the absence of ligand.

The use of a “heterodimer” technique to probe questions of allostery in caspases specifically, and proteases in general, is not without precedent. Recent work by Denault and colleagues used engineered caspase-7 heterodimers where only one of the subunits was rendered catalytically inactive by mutagenesis. This study observed that the activity of the resulting caspase-7 heterodimer was half that of wild type, suggesting that the unaltered catalytic site maintained full activity and that the two catalytic domains in the caspase-7 dimer are equal and independent (Denault, Bekes et al. 2006). Based on our results using the hybrid caspase-3 heterodimer, we would predict that caspase-7, also an executioner caspase, would reside predominantly in the active conformation and not show coupling between active sites. The work by Denault and colleagues seems to support that prediction.

HIV protease is another protease that like caspases exists as a homodimer in its active form. In a study presented by Rozzelle and colleagues, HIV protease was engineered with three point mutations to create a dominant-negative inhibitor of wild type HIV protease. This inhibitor acts by forming a heterodimer with wild type HIV protease and inhibiting its activity (Rozzelle, Dauber et al. 2000). Because of the functional coupling we see between the two subunits of the caspase-1 dimer, it would be interesting to test whether a caspase-1 heterodimer could be generated where an inactive subunit could inhibit the activity of the active subunit. This would stand in marked contrast to the result in caspase-7 described above.

In fact, previous reports have described a dominant-negative effect of a mutated caspase-1 construct. Friedlander and colleagues created an active-site caspase-1 mutant by knocking out the catalytic cysteine with a C285G mutation. This variant was then expressed in a transgenic mouse model under the control of a neuron-specific promoter. They were able to show that expression of this caspase-1 variant protected neurons from apoptosis following

trophic factor withdrawal and reduced brain injury following ischemic events (Friedlander, Gagliardini et al. 1997). A subsequent study showed that expression of the same caspase-1 dominant-negative mutant in a mouse model of Huntington's disease delayed symptoms and prolonged survival (Ona, Li et al. 1999). The molecular mechanism by which this caspase-1 mutant is able to exert a dominant-negative effect has not been elucidated, but it would be interesting to test this mutant using our method for engineering a hybrid heterodimer.

The elucidation of the differences in conformational state and allosteric regulation between inflammatory and executioner caspases raises questions as to what the biological significance of these observations could be. The inflammatory and apoptotic pathways share very similar molecular elements. Both can be activated by extracellular and intracellular receptors that sense danger signals, both involve scaffolding proteins and the formation of macromolecular complexes, and both pathways are crucially dependent on proteolytic events. However, the end result of the two pathways is very different. In the case of inflammatory signaling and caspase-1 activation, this pathway leads to the release of inflammatory cytokines from the cell and subsequent activation of immune cells. In contrast, the apoptotic pathway and caspase-3 activation leads to the programmed cell death of the cell in which the pathway is activated.

Recent studies have taken a proteomic approach to globally profile proteolytic cleavage products following induction of various caspase pathways. These studies have shown that the number of potential caspase substrates during inflammatory signaling is small, on the order of thirty (Agard, Maltby et al. 2010). Our observation that caspase-1 resides in an inactive conformation suggests that positive cooperativity may provide an additional selectivity filter for cleaving pro-inflammatory substrates only when they are concentrated in cells. It has been

recently suggested that caspase-1 cleaves pro-IL-1β that has been concentrated at membranes, in inflammasomes, or in vesicles (MacKenzie, Wilson et al. 2001; Andrei, Margiocco et al. 2004; Ferrari, Pizzirani et al. 2006). However, in apoptotic signaling events, the potential number of caspase substrates is on the order of a thousand (Mahrus, Trinidad et al. 2008). Given these observations, it seems to make sense that the executioner caspase-3 would reside in a more active conformation in comparison to caspase-1. The apoptotic pathway, which results in a vast number of substrates being cleaved and the dismantling of a cell requires a very active protease, whereas the inflammatory pathway, with few substrates cleaved in a specific cytokine signaling event, seems to call for a protease under much tighter regulation. Our model provides a mechanism by which the very conformational state of the various caspase family members recapitulates their role in specific biologic pathways and provides an additional level of regulation.

3.9 Experimental Procedures

3.9.1 Expression and purification of caspase-1

Recombinant caspase-1 was prepared by expression in *Escherichia coli (E. coli)* as insoluble inclusion bodies followed by refolding (Romanowski, Scheer et al. 2004; Scheer, Wells et al. 2005). The p20 (residues 120 – 297) and p10 (residues 317 – 404) subunits of wild type human caspase-1 were cloned into NdeI and EcoRI restriction endonuclease sites of the pRSET plasmid (Invitrogen, Carlsbad, CA). Site-directed mutagenesis was performed using the QuikChange Site-Directed Mutagenesis Kit from Stratagene (La Jolla, CA).

Caspase-1 subunits were expressed separately in *E. coli* BL21(DE3) Star cells (Invitrogen). Cells were harvested following induction of a log phase culture with 1mM IPTG for 4 h at 37°C

and then disrupted with a microfluidizer. The inclusion body pellets were isolated by centrifugation of lysate for 20 min at 4°C. Pellets were washed twice with 50 mM HEPES (pH 8.0), 300 mM NaCl, 1 M guanidine-HCl, 5 mM DTT, and 1% Triton X-100, and washed two more times with the same buffer without the detergent. The washed inclusion body pellets were solubilized in 6 M guanidine-HCl and 20 mM DTT, and stored frozen at -80°C.

Refolding of caspase-1 was done by combining guanidine-HCl-solubilized large and small subunits (10mg of large subunit and 20mg of small subunit) in a 250 mL beaker, followed by rapid dilution with 100 mL of 50 mM HEPES (pH 8.0), 100 mM NaCl, 10% sucrose, 1 M nondetergent sulfobetaine 201 (NDSB-201), and 10 mM DTT. Renaturation proceeded at room temperature for 6 h. Samples were centrifuged at 16,000 g for 10 minutes to remove precipitate, and then dialyzed overnight at 4°C against 50 mM sodium acetate (pH 5.9), 25 mM NaCl, 5% glycerol, and 4 mM DTT. Dialyzed protein was purified by cation exchange chromatography using a pre-packed 5 mL HiTrap SP HP column (GE Healthcare Bio-sciences Corp, Piscataway, NJ). Protein was eluted using a linear gradient of 0-1.0 M NaCl over 20 min in a buffer containing 50 mM sodium acetate (pH 5.9) and 5% glycerol. Peak fractions were pooled and β-ME was added to a concentration of 1mM before samples were stored frozen at -80°C.

3.9.2 Active site titration

Protein concentration for enzyme kinetic analysis was determined by active-site titration (Stennicke and Salvesen 1999); caspase was incubated in assay buffer for 2 hrs at room temperature with a titration from a zero- to 2-fold stoichiometric ratio using the irreversible active-site inhibitor z-VAD-FMK. The protein was diluted to an enzyme concentration of 50 nM and activity was determined using fluorogenic tetrapeptide substrate (Axxora, San Diego, CA)

at 25 μM for caspase-1 or 50 μM for caspase-3. The substrates used were Ac-WEHD-AFC for caspase-1 constructs and Ac-DEVD-AFC for caspase-3 constructs (Rano, Timkey et al. 1997; Talanian, Quinlan et al. 1997; Thornberry, Rano et al. 1997).

3.9.3 Expression and purification of half-labeled caspase constructs

The generation of hybrid caspase-1 and caspase-3 constructs follows the protocol described above. Caspase-1 (residues 120-297) and caspase-3 (residues 29-175) large subunits containing an N-terminal His_6- or Strep-affinity tags were generated by designing 5'- primers with the appropriate sequence for the affinity tag and using polymerase chain reaction (PCR) to generate dsDNA inserts. The affinity-tag amino acid sequences were "MRGSHHHHHHSAG-" for the His_6-tagged construct and "MWSHPQFEKSAG-" for the Strep-tagged construct. The Strep-tag is an eight amino acid peptide that binds with high selectivity to the streptavidin variant Strep-Tactin (IBA GmbH, Germany). These inserts were sub-cloned into NdeI and EcoRI restriction endonuclease sites of the pRSET plasmid (Invitrogen, Carlsbad, CA). The p10 small subunit of caspase-1 (residues 317 – 404) and the p17 small subunit of caspase-3 (residues 176 – 277) were also cloned into the pRSET plasmid. These constructs were then expressed and purified as inclusion body pellets as described above. In addition, full-length caspase-3 constructs (residues 1-277) containing N-terminal affinity tags were generated using the above 5'- primer and then sub-cloned into NdeI and EcoRI restriction endonuclease sites of the pET-23b plasmid (Novagen). This construct was used for soluble expression of caspase-3.

3.9.3.1 Expression and purification of half-labeled caspase-1

To generate the half-labeled caspase-1 construct, active caspase-1 was first generated by refolding a His_6- or Strep-tagged large subunit with the small subunit to generate the active caspase dimer, as described above. Following refolding, samples were centrifuged at 16,000 g for 10 minutes to remove precipitate, diluted two-fold into 50 mM sodium acetate (pH 5.9) buffer, and then centrifuged once more at 16,000 g for 10 minutes. Samples were filtered and purified by cation exchange chromatography.

The tagged caspase-1 construct was then labeled with the irreversible active site inhibitor z-VAD-FMK in labeling buffer containing 50 mM HEPES (pH 7.4), 50 mM KCl, 200 mM NaCl, and 10 mM DTT overnight at 4°C. Complete labeling of the tagged p20 subunit was verified by liquid chromatography-mass spectrometry (LC-MS; Waters, Milford, MA) and complete inhibition of catalytic activity. Excess inhibitor was removed using a Superdex 200 10/300 gel filtration column (GE Amersham) in buffer containing 25 mM Tris (pH 8.0), 50 mM NaCl, 5% glycerol, and 1mM DTT. The VAD-FMK-labeled tagged caspase-1 was then concentrated using Millipore Ultrafree-15 devices with a MWCO of 10,000 Da and then denatured in 6M guanidine. This sample was then refolded in the presence of the other tagged p20 subunit and excess p10 subunit. Refolding and purification by cation exchange chromatography were done as described above. The three affinity-tagged caspase-1 species were then separated using sequential 1mL HisTrap and 1mL StrepTrap columns for affinity purification (GE Healthcare), and the final half-labeled caspase-1 construct was purified by size exclusion chromatography using a Superdex 200 16/60 column in 25 mM Tris (pH 8.0), 50 mM NaCl, 5% glycerol, and 1mM DTT. Final verification of sample purity as being properly half-labeled was performed by LC-MS.

The control heterodimer caspase-1 with both His_6- or Strep-affinity tags but no labeling with the active-site inhibitor VAD-FMK was generated in a similar fashion as above. Three caspase-1 constructs, the His_6-tagged p20, Strep-tagged p20, and p10 subunits from inclusion bodies were refolded together, then purified as above using cation exchange chromatography, sequential His_6- and Strep-tag affinity based purification, and finally size exclusion chromatography.

3.9.3.2 Expression and purification of half-labeled caspase-3

To generate the half-labeled caspase-3 construct, active caspase-3 was first generated by soluble expression in *E. coli* BL21(DE3)pLysS cells (Stratagene). Cells were grown in 2xYT media containing 200 µg/ml ampicillin and 50 µg/ml chloramphenicol at 37 °C to an OD600nm of 0.8-1.0. Overexpression of caspase-3 was induced with 200 µM IPTG at 37°C for three hours. Cells were harvested and resuspended in 100 mM Tris (pH 8.0) and 100 mM NaCl for lysis by microfluidization (Microfluidics). The cell lysate was spun at 45,000xg for 30 minutes at 4°C. Caspase-3 with an N-terminal His_6-affiniy tag was isolated using a 1 ml HisTrap HP Ni-NTA affinity column (GE Amersham) eluted with buffer containing 200 mM imidazole. The eluted protein was diluted two-fold with buffer containing 20 mM Tris, pH 8.0 and then purified by anion-exchange chromatography (HiTrap Q HP, GE Amersham) with 30-column volume gradient from 0-0.5 M NaCl.

The His_6-affiniy tagged caspase-3 construct was then labeled and purified with the irreversible active site inhibitor z-VAD-FMK as described above for caspase-1. Following refolding with Strep-affinity tagged p17 large subunit and p12 small subunit, samples were dialyzed overnight at 4°C against 20 mM Tris (pH 5.9), 1 mM DTT. Dialyzed protein was purified

by anion-exchange chromatography as described above. The three affinity-tagged caspase-3 species were then separated using sequential 1mL HisTrap and 1mL StrepTrap affinity purification (GE Healthcare), and the final half-labeled caspase-3 construct was purified using a Superdex 200 16/60 gel filtration in 20 mM Tris (pH 8.0), 50 mM NaCl, and half-labeling was verified by LC-MS.

The control heterodimer caspase-3 with both His_6- or Strep-affinity tags but no labeling with the active-site inhibitor VAD-FMK was generated in a similar fashion as above. Three caspase-3 constructs, the His_6-tagged p17, Strep-tagged p17, and p12 subunits from inclusion bodies were refolded together, and then purified as above using anion exchange chromatography, sequential His_6- and Strep-tag affinity based purification, and finally size exclusion chromatography.

3.9.4 Enzyme kinetic analysis

For kinetic analysis of caspase-1, protein was buffer exchanged using a NAP-5 Column (Amersham) into assay buffer containing 50 mM HEPES (pH 8.0), 50 mM KCl, 200 mM NaCl, 10 mM DTT, 0.1% 3-[(3-cholamidopropyl)dimethylammonio]-1-propanesulfonate (CHAPS). Kinetic analysis of caspase-3 was performed in buffer containing 50 mM HEPES (pH 7.4), 50 mM KCl, 0.1 mM EDTA, 1 mM DTT and 0.1% CHAPS. Steady-state kinetic analysis was done by titrating enzyme with fluorogenic tetrapeptide substrate (Ac-WEHD-AFC for caspase-1 constructs and Ac-DEVD-AFC for caspase-3 constructs; Axxora, San Diego, CA) typically from 200 μM to 0.25 μM. The enzyme concentration was set to 50 nM for all variants except for the caspase-1 G287A variant (500 nM) that showed a large decrease in activity. Kinetic data was collected for a 10 min

time course using a Spectramax M5 microplate reader (Molecular Devices, Sunnyvale, CA) with excitation, emission, and cutoff filters set to 365 nm, 495 nm, and 435 nm, respectively.

Kinetic constants V_{max}, K_M, and the Hill coefficient (n_{Hill}) were calculated using GraphPad PRISM. The initial velocity (*v)*, measured in relative fluorescence units per unit time, was plotted versus the logarithm of substrate concentration. The model used to fit the data is a sigmoidal does-response curve with variable slope, and from this model all three kinetic constants were derived. The general equation of this model is Y = Bottom + (Top-Bottom)/(1+10^((LogEC_{50}-X)*HillSlope)), where Y is the initial velocity, X is the logarithm of the substrate concentration, and Top, Bottom, EC_{50} (K_M), and Hill Slope are free parameters fit to the data. A standard curve using pure AFC product was used to convert relative fluorescence units to units of concentration (μM). In determining kinetic constants for caspases we observed that at saturating substrate concentrations, the enzyme exhibited decreasing activity as substrate concentration increased, most likely due to substrate inhibition. In order to correctly fit our data using non-linear regression, data points exhibiting product inhibition were excluded.

3.9.5 Kinetic analysis by surface plasmon resonance

Conformation-specific antibodies (Fabs) were expressed as described (Gao, Sidhu et al. 2009) and purified using protein A affinity chromatography. Kinetic binding analysis of Fabs to caspase-1 was performed by surface plasmon resonance (SPR) using a BIACore T100 (GE Healthcare). Caspase-1 dimer constructs were immobilized on CM5 chips using a standard amine coupling kit (GE Healthcare; 1-ethyl-3-(3-dimethylaminopropyl) carbodiimide hydrochloride (EDC), N-hydroxysuccinimide (NHS), ethanolamine-HCl pH 8.5). Serial dilutions of Fabs were injected in HEPES buffered saline, pH 7.4 plus 0.05% Tween20. Binding responses in

flow cells containing immobilized caspase-1 constructs were corrected by subtraction of responses in a blank reference flow cell. The BIAevaluation software (GE Healthcare) was used for fitting sensograms utilizing a 1:1 Langmuir model, and K_D values were calculated using the ratio of k_{off}/k_{on}.

3.10 References

Agard, N. J., D. Maltby, et al. (2010). "Inflammatory stimuli regulate caspase substrate profiles." Mol Cell Proteomics **9**(5): 880-93.

Andrei, C., P. Margiocco, et al. (2004). "Phospholipases C and A2 control lysosome-mediated IL-1 beta secretion: Implications for inflammatory processes." Proc Natl Acad Sci U S A **101**(26): 9745-50.

Cerretti, D. P., C. J. Kozlosky, et al. (1992). "Molecular cloning of the interleukin-1 beta converting enzyme." Science **256**(5053): 97-100.

Datta, D., J. M. Scheer, et al. (2008). "An allosteric circuit in caspase-1." J Mol Biol **381**(5): 1157-67.

Denault, J. B., M. Bekes, et al. (2006). "Engineered hybrid dimers: tracking the activation pathway of caspase-7." Mol Cell **23**(4): 523-33.

Ferrari, D., C. Pizzirani, et al. (2006). "The P2X7 receptor: a key player in IL-1 processing and release." J Immunol **176**(7): 3877-83.

Friedlander, R. M., V. Gagliardini, et al. (1997). "Expression of a dominant negative mutant of interleukin-1 beta converting enzyme in transgenic mice prevents neuronal cell death induced by trophic factor withdrawal and ischemic brain injury." J Exp Med **185**(5): 933-40.

Gao, J., S. S. Sidhu, et al. (2009). "Two-state selection of conformation-specific antibodies." Proc Natl Acad Sci U S A **106**(9): 3071-6.

Grutter, M. G. (2000). "Caspases: key players in programmed cell death." Curr Opin Struct Biol **10**(6): 649-55.

Hardy, J. A., J. Lam, et al. (2004). "Discovery of an allosteric site in the caspases." Proc Natl Acad Sci U S A **101**(34): 12461-6.

Jiang, J., X. Wang, et al. (2004). "A conformationally sensitive GHR [growth hormone (GH) receptor] antibody: impact on GH signaling and GHR proteolysis." Mol Endocrinol **18**(12): 2981-96.

Li, R., I. Haruta, et al. (2002). "Characterization of a conformationally sensitive murine monoclonal antibody directed to the metal ion-dependent adhesion site face of integrin CD11b." J Immunol **168**(3): 1219-25.

Lovell, S. C., I. W. Davis, et al. (2003). "Structure validation by Calpha geometry: phi,psi and Cbeta deviation." Proteins **50**(3): 437-50.

MacKenzie, A., H. L. Wilson, et al. (2001). "Rapid secretion of interleukin-1beta by microvesicle shedding." Immunity **15**(5): 825-35.

Mahrus, S., J. C. Trinidad, et al. (2008). "Global Sequencing of Proteolytic Cleavage Sites in Apoptosis by Specific Labeling of Protein N Termini." Cell.

Martinon, F. and J. Tschopp (2007). "Inflammatory caspases and inflammasomes: master switches of inflammation." Cell Death Differ **14**(1): 10-22.

Ona, V. O., M. Li, et al. (1999). "Inhibition of caspase-1 slows disease progression in a mouse model of Huntington's disease." Nature **399**(6733): 263-7.

Pray, T. R., K. K. Reiling, et al. (2002). "Conformational change coupling the dimerization and activation of KSHV protease." Biochemistry **41**(5): 1474-82.

Rano, T. A., T. Timkey, et al. (1997). "A combinatorial approach for determining protease specificities: application to interleukin-1beta converting enzyme (ICE)." Chem Biol **4**(2): 149-55.

Romanowski, M. J., J. M. Scheer, et al. (2004). "Crystal structures of a ligand-free and malonate-bound human caspase-1: implications for the mechanism of substrate binding." Structure **12**(8): 1361-71.

Rozzelle, J. E., D. S. Dauber, et al. (2000). "Macromolecular inhibitors of HIV-1 protease. Characterization of designed heterodimers." J Biol Chem **275**(10): 7080-6.

Scheer, J. M., M. J. Romanowski, et al. (2006). "A common allosteric site and mechanism in caspases." Proc Natl Acad Sci U S A **103**(20): 7595-600.

Scheer, J. M., J. A. Wells, et al. (2005). "Malonate-assisted purification of human caspases." Protein Expr Purif **41**(1): 148-53.

Stennicke, H. R. and G. S. Salvesen (1999). "Caspases: Preparation and characterization." Methods **17**(4): 313-319.

Talanian, R. V., L. C. Dang, et al. (1996). "Stability and oligomeric equilibria of refolded interleukin-1beta converting enzyme." J Biol Chem **271**(36): 21853-8.

Talanian, R. V., C. Quinlan, et al. (1997). "Substrate specificities of caspase family proteases." J Biol Chem **272**(15): 9677-82.

Thornberry, N. A., H. G. Bull, et al. (1992). "A novel heterodimeric cysteine protease is required for interleukin-1 beta processing in monocytes." Nature **356**(6372): 768-74.

Thornberry, N. A., T. A. Rano, et al. (1997). "A combinatorial approach defines specificities of members of the caspase family and granzyme B. Functional relationships established for key mediators of apoptosis." J Biol Chem **272**(29): 17907-11.

Chapter 4:

Conclusion and Future Directions

4.1 Conclusion

The studies presented in this dissertation provide a variety of evidence demonstrating the importance of allostery in the function of caspases. Using site-directed mutagenesis, we have shown the central role of a salt bridge interaction in caspase-1 and how these residues constitute an allosteric circuit connecting the two active sites of the caspase-1 homodimer. We have also shown how targeting specific glycine and proline residues in caspase-1 selects for different conformational states of the enzyme. Lastly, our experiments with covalent inhibitors for caspases have demonstrated the utility of chemical ligands for trapping conformational states of proteins and understanding how allostery plays a role in caspase activity.

Many avenues remain to be explored in elucidating mechanisms of caspase activation and regulation. This chapter presents some preliminary data and proposals for future experiments that could broaden understanding of this important family of proteases.

4.2 Engineering a salt-bridge into the executioner caspase-7

Our mutational analysis of the hydrogen bonding network in caspase-1 demonstrated the importance of a central salt bridge interaction between Arg286 and Glu390. The presence of an arginine at position 286 appears to be essential; even a slight variation to a lysine at this position resulted in over hundred-fold reduction in activity. The presence of an acidic residue to coordinate with the arginine is also important. Mutation of the glutamate to an alanine at position 390 results in a reduction of activity similar to mutation of the arginine, but switching acidic residues from a glutamate to an aspartate seems to be well tolerated at this position.

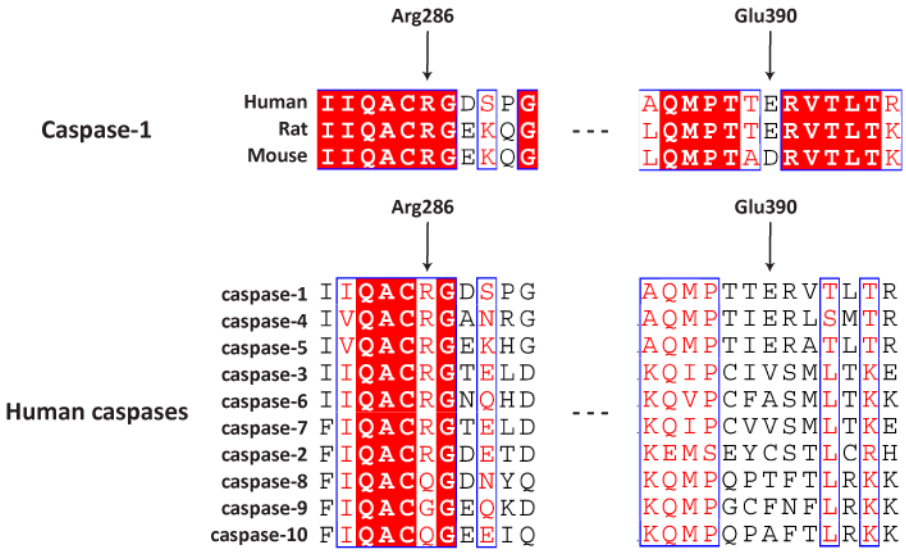

Figure 4.1. Sequence alignments of caspase-1 in mammals and human caspases. (Top) The sequence alignment of caspase-1 from human, rat, and mouse demonstrates full conservation of Arg286 and conservation of an acidic residue at position 390. **(Bottom)** Sequence alignment of ten human caspases shows that the Arg286-Glu390 salt bridge is only preserved among inflammatory caspases-1, -4, and -5. Caspase-7, an executioner caspase, contains arginine at position 286, but has a valine at the 390 position instead of an acidic residue as in caspase-1.

The importance of the salt bridge residues for caspase-1 activity raises questions about the possible importance of this type of interaction for other caspases. Sequence alignments of the caspase-1 protein from human, rat, and mouse show that Arg286 is completely conserved, as is an acidic residue at position 390; the mouse caspase-1 contains aspartate instead of glutamate at this position, but our mutational analysis would suggest that this variation has a very small effect on enzyme activity (Figure 4.1). Based on the sequence conservation we predict that the salt bridge interaction is likely preserved in rat and mouse caspase-1 (only the human homolog has been crystallized).

A comparison of the sequences of 10 of the human caspases indicates that the salt bridge interaction is not fully conserved across the caspase family. Only the three inflammatory caspases (caspase-1, -4, and -5) contain both an arginine at position 286 and a glutamate at

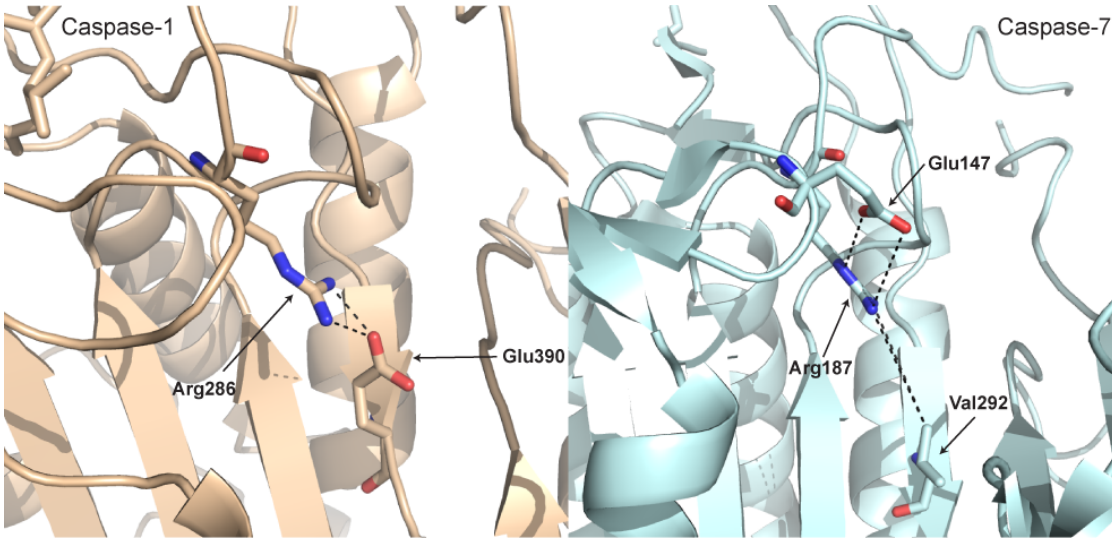

Figure 4.2. Structural comparison of caspase-1 and caspase-7. (Left) Caspase-1 contains a salt bridge formed by Arg286 and Glu390. **(Right)** Caspase-7 contains an arginine (Arg187) at the position corresponding to Arg287 in caspase-1. The amino acid position occupied by Glu390 in caspase-1 is occupied by Val292 in caspase-7. The Arg187 in caspase-7 appears to be able to form polar interactions with the neighboring Glu147. Caspase-1 does not have an acidic residue at the corresponding position.

position 390 (Figure 4.1). The executioner caspases (caspase-3, -6, -7) all have the arginine at position 286, but these enzymes have a valine or alanine at position 390. Of the initiator caspases, only caspase-2 contains an arginine at position 286; caspase-8 and -10 contain glutamine while caspase-9 has a glycine. None of the four initiator caspases has an acidic residue at position 390. The sequence alignment suggests that the salt-bridge interaction is only conserved for the inflammatory caspases in humans, and available crystal structures support this prediction.

However, given the large impact of perturbations in the salt bridge for caspase-1, we wondered whether the activity of an executioner caspases could be increased by engineering in a salt bridge interaction. We decided to test this in the caspase-7 system. Figure 4.2 shows a comparison between the structures of the Arg286-Glu390 salt bridge in caspase-1 and the

corresponding residues in caspase-7. The arginine half of a potential salt bridge is present in caspase-7 (Arg187) as in all executioner caspases, but appears to interact with a nearby acidic residue (Glu147) that is not present in caspase-1 at that position. The Glu390 position in caspase-1 is occupied by Val292 in caspase-7. Therefore, our strategy for engineering a salt bridge into caspase-7 involves mutating Val292 to an acidic residue to form the salt bridge interaction and mutating out Glu147 to prevent a potential competing interaction.

We used site-directed mutagenesis to mutate Glu147 to an alanine and Val292 to either a glutamate or aspartate. We tried all 5 possible combinations of mutations, and then tested the enzyme activity of each variant. As shown in Table 4.2, none of the variants we tested showed significant differences in catalytic efficiency as compared to wild type caspase-7. Any combination of mutations resulted in less than two-fold changes in caspase-7 activity. Therefore, the presence or absence of a potential engineered salt-bridge has little effect on the activity of caspase-7, in stark contrast to the central importance of this type of interaction for caspase-1 activity.

What could explain this difference between the inflammatory caspase and the executioner caspase? These experiments in caspase-7 were carried out prior to our half-labeling experiment with the related executioner caspase, caspase-3. At the time, we did not have direct evidence demonstrating that caspase-3 is in an active conformation in solution. Our current model of the conformational state of caspases based on those studies predicts that caspase-1 normally resides in an inactive state, whereas executioner caspases, like caspase-3 and -7, normally reside in an active state. This difference in conformational states explains the difference in importance we find for the presence of the salt bridge in caspase-1 versus caspase-7. Caspase-1 appears to require the salt bridge interaction to stabilize its active conformation.

Table 4.1. Caspase-7 variants engineered for a salt-bridge have activity similar to wild type.

Construct	K_M μM	k_{cat} sec^{-1}	k_{cat}/K_M, $M^{-1}\bullet sec^{-1}$	Ratio k_{cat}/K_M
Wild type caspase-7	56	4.7	8.0×10^4	1
E147A	52	3.7	7.1×10^4	0.89
V292D	50	4.0	8.6×10^4	1.09
V292E	46	3.7	1.0×10^5	1.29
E147A / V292D	37	3.3	6.9×10^4	0.87
E147A / V292E	48	3.9	7.7×10^4	0.97

*Standard errors within 10% of reported values based on data collected in triplicate.

Without it, the catalytic activity of the protease is greatly reduced. Conversely, caspase-7 already resides in the active conformation, so the presence of a newly engineered salt bridge can do little to further stabilize an already stable conformational state.

4.3 The dimer nature of caspases and protease processivity

It is unusual for proteases to be dimers, let alone demonstrate positive cooperativity, and this observation raises interesting questions as to whether there is functional relevance to these properties of caspases in the context of their biological function. In this section, we propose future studies that will attempt to address this and other important outstanding questions on allostery in caspases. We have already shown how the dimer nature of caspase-1 allows for positive cooperativity and the activation of one subunit by active-site labeling of the other subunit. We present here experiments whose aim is to further characterize the importance of the dimer nature of caspases.

4.3.1 A nanoparticle model to test processive protease activity of protein complexes

The observation that caspases, unlike most other proteases, are dimers, and in the case of caspase-1, demonstrate cooperativity, raises questions as to whether there is any functional relevance to these properties. Positive cooperativity in caspase-1 suggests that this protease will prefer to cleave substrates found at high concentration, such as those that are localized to specific compartments of the cell or those found in complexes. Caspase-3 does not show cooperativity in our *in vitro* enzyme assays, yet the fact remains that it is a dimer and this is unusual for proteases. In a recent study, global profiling of proteolytic cleavage products following induction of apoptosis found the surprising result that a disproportionate number of caspase substrates physically interact. This suggests that executioner caspases may preferentially target protein complexes and networks (Mahrus, Trinidad et al. 2008). Is it possible that the dimeric nature of caspases is important for the preferential cleavage of substrates in complexes, and perhaps permits the protease to cleave complexes in a processive manner?

One of the complexes identified as a target for caspase cleavage during apoptosis is the N-CoR/SMRT transcriptional corepressor complex. This complex is involved in the regulation of chromatin condensation and transcription through the recruitment of histone deacetylases. Components of this complex that have been found to be targets of caspase activity include N-CoR, SMRT, HDAC-3, HDAC-7, SHARP, TBLR1, and RBBP7 (Escaffit, Vaute et al. 2007; Karagianni and Wong 2007; Mahrus, Trinidad et al. 2008). The cleavage sites identified in these components appear to lie between functional domains, suggesting that proteolysis of members of the complex leads to its inactivation by allowing these domains to fall apart. This may have a physiological consequence similar to HDAC inhibitors, which cause decreased histone

deacetylation allowing chromatin to open, ultimately resulting in upregulation of proapoptotic genes (Bolden, Peart et al. 2006; Mahrus, Trinidad et al. 2008). Interestingly, the caspase cleavage site in each of the components of this complex contains a different amino acid sequence. This raises the question as to whether the cleavage sequence itself may have an effect on the order or speed at which proteolysis occurs. One could imagine that the "best" caspase cleavage site attracts the initial caspase proteolytic event and other, less optimal sites in the complex are then cleaved in a processive fashion.

In order to address these questions, we propose to test the activity of caspase-1 and -3 in a gold nanoparticle model of protein complexes. Gold nanoparticles are nanometer-scale (~ 40-nm) and efficiently scatter light without blinking or photobleaching. The optical properties of these particles are dependent on plasmons, which are the collective oscillations of conduction electrons. The wavelength of emitted light can be controlled by altering the size and shape of the nanoparticles. Plasmons from different particles also couple in a distance-dependent manner, meaning that the nanoparticles get brighter as they are brought closer together. Therefore, these can be used to monitor changes in distance on the nanometer scale, much like in FRET, except without the issues of blinking and photobleaching. The coupling between nanoparticles is also brighter and has a better signal-to-noise ratio than with FRET fluorophore dyes (Reinhard, Sheikholeslami et al. 2007). Imaging of these particles involves illumination by unpolarized white light, and scattered light from the particles is collected by transmission darkfield microscopy (Sonnichsen, Reinhard et al. 2005).

Our model of protein complexes involves linking gold nanoparticles together with short peptide linkers containing caspase cleavage sequences. When these peptides are cleaved, it causes the linked nanoparticle to fall out of the complex, since these particles repel each other

in low ionic strength environments (Sonnichsen, Reinhard et al. 2005). This can be monitored by measuring the intensity of scattered light, which drops when the particles move apart. These single particle events can be measured in real-time, allowing us to monitor the time course of proteolysis events in a single gold nanoparticle complex.

This experiment will involve synthesizing gold nanoparticle complexes that contain anywhere from 3-6 “satellite” nanoparticles attached to a central nanoparticle by identical peptide linkers containing the caspase-1 cleavage sequence WEHD. On one end, the peptide linker is biotinylated, and this binds to the central nanoparticle which is coated in avidin. On the other end, the linker is terminated by two cysteine residues, which allows attachment to a satellite nanoparticle through gold-thiolate bonds. We could then add either wild type caspase-1 or our half-labeled construct to the particles and monitor cleavage events. Our hypothesis is that wild type caspase-1 will cleave these complexes in a cooperative and processive fashion; the hybrid construct will be unable to do so since one of its active sites is blocked. Therefore, we expect the hybrid to cleave the complexes as if it were a monomer protease.

What would these different activities look like in the data? One thing to note is that though we do not expect the half-labeled hybrid to show cooperativity or processivity, its basal level of protease activity is 10-fold higher than wild type. So the first thing we might expect is that the absolute rate of cleavage events is higher for the hybrid construct. However, the wild type protease could cleave complexes cooperatively and with processivity. Since all the substrate targets are localized in complexes, we may find that the cooperative wild type caspase-1 is better than the hybrid construct at cleaving substrates in this setting.

Since we cannot monitor the caspase itself, only its cleavage events in this system, we will need to measure the properties of cooperativity and processivity based on the time course

of cleavages of individual complexes. Since wild type caspase-1 is cooperative, for single complexes we would expect that complete cleavage of all the linkers would go to completion faster than for the half-labeled enzyme once an initial cleavage event takes place. In other words, the total time it takes from the initial to final cleavage event for a single complex should be shorter for wild type than for the half-labeled hybrid construct.

Processivity for a caspase in this context can be defined as the number of cleavage events that occur on a given complex before the enzyme dissociates and moves on to another complex. Therefore, in the population of complexes as a whole, we would expect that entire complexes fall apart one by one with wild type caspase-1, whereas with the half-labeled hybrid we may see a more gradual decrease in the intensity of each of the complexes. In other words, wild type caspase-1 should cause the complexes to turn off like light bulbs, whereas the half-labeled construct should cause the light bulbs to dim gradually. Another value that we can measure in the data is the lag time before a complex starts to be cleaved. For example, wild type caspase-1 will likely completely dissociate a single complex before moving on to the next. Therefore, across the entire population of complexes we would expect to see a broad distribution of lag times before the initial cleavage. However, the half-labeled construct would not cut processively, and could therefore move quickly between complexes making single cuts in each one. In this case, we would expect to see the distribution of lag times skewed to smaller values.

It would be informative to repeat the above experiment for caspase-3, and its corresponding half-labeled hybrid construct. We will need to create new peptide linkers with DEVD cleavage sequences that are preferred by this protease. As in the case of caspase-1, we will compare the cleavage of substrates for wild type caspase-3 versus the half-labeled hybrid

construct. We hypothesize that caspase-3 already sits in the active conformation since it does not show positive cooperativity. Therefore, we may not see as great a difference in the cooperative cleavage of complexes, but we may still see a difference in processive cleavage of the complexes between the dimer wild type and the half-labeled construct. Of course, it will also be interesting to compare the data between caspase-1 and caspase-3 to see if differences in cooperativity between these enzymes manifest in a difference in cleavage of the complexes.

In order to get a sense for what proteolysis by a true monomer protease looks like in our model, we will use trypsin as a control. Since this enzyme is a monomer, it should show neither cooperativity, nor processivity when cleaving complexes. The substrate specificity of trypsin is for arginine in the P1 position so long as P1' is not proline. Therefore, we can easily include trypsin cleavage sites in our peptide linkers by ensuring that they contain an arginine that is not followed by a proline, and use trypsin as a control monomer protease in this system.

We would also like to address whether the amino acid sequence of a caspase cleavage site has a functional effect on the order in which components of a complex are cleaved. This experiment would take advantage of the fact that the intensity of scattered light between two nanoparticles scales not only with the distance between them, but also with the size of the particles. Therefore, a larger particle falling off the complex will create a bigger change in scattered light intensity than a smaller particle. We could construct various peptide linkers with different caspase cleavage sequences corresponding to the cleavage sites of proteins in our complex of interest, the N-CoR/SMRT complex. We can then create unique peptide-nanoparticle pairs where a specific cleavage sequence is linked to a satellite nanoparticle of a specific size. Protein complexes with various cleavage sequences could be made, and we could then

determine which cleavage event is taking place from the magnitude of the intensity change of the scattered light.

There are two important controls that would need to be done to check for artifacts in this experiment. First, we would need to ensure that particle size alone does not affect the order of cleavage events. For example, one could imagine it is easier for caspase-3 to cleave next to a smaller particle. Therefore, we should create complexes with different size nanoparticles as in the experiment above, but all with the same DEVD cleavage sequence in each of the linkers. Second, we should measure the individual rates of cleavage for each of the peptide sequences we are interested in. To do this we can construct quenched fluorogenic test octopeptides (containing the P4 through P4' cleavage sequence) that are labeled with the FRET pair DABCYL at the N-terminus and EDANS at the C-terminus. Cleavage of the peptide will separate the fluorophore (EDANS) from its quencher (DABCYL), and the resulting increase in fluorescence can be measured to determine the various rate of proteolysis for a given peptide substrate (Matayoshi, Wang et al. 1990; Maggiora, Smith et al. 1992).

This experimental setup allows us to ask some interesting questions. First, is the order of cleavage events in a complex determined by the cleavage sequence itself? We can compare the rates of cleavage of the test quenched peptides to the order in which the sequences are cleaved in the complexes. Second, we can ask, does the presence of certain sequences make it easier for other sequences to be cleaved? One might expect this to be the case if the dimer nature of caspase-3 allows it to cleave substrates in the complex processively. We can then compare the half-labeled dimer in this situation and check for differences for a non-processive protease. As part of this experiment, we could include the canonical caspase-3 cleavage sequence DEVD in the complex. We expect that since this synthetic peptide sequence results in

the best caspase-3 kinetics *in vitro*, in will preferentially be cut first in the nanoparticle complexes. We may also find that the presence of this cleavage sequence improves the ability of wild type caspase-3 to cleave other, less optimal sequences in the same complex. If this is the case, it would be especially interesting to see whether our half-labeled hybrid construct would lose this ability.

4.3.2 Analyzing processive caspase-3 activity in the cleavage of a protein complex

The next part of the proposed studies attempts to address the question of whether cooperativity and processivity in caspases are important for the cleavage of an actual biological complex. As described above, multiple components of the N-CoR/SMRT complex are cleaved by caspases following the induction of apoptosis. Interestingly, the various components have different sequences at their caspase cleavage site, and based on the amino acid sequences of these sites, we would expect that some of these may not be "ideal" for caspase recognition and activity (Mahrus, Trinidad et al. 2008). However, caspases are dimers, and this could conceivably permit the two active sites to interact with two different cleavage sites in the same complex. This raises the question as to whether the presence of one cleavage site is important for cleavage of neighboring, less optimal sites in the complex. In order to address this issue, we intend to test and compare the activity of wild type caspase-3 and our half-labeled caspase-3 against the purified N-CoR/SMRT complex.

Our first goal would be to isolate the N-CoR/SMRT complex from nuclear extracts of Hela cells, as described in work by Yoon and colleagues (Yoon, Chan et al. 2003). Briefly, the purification method involves multiple chromatographic steps involving cation and anion exchange, followed by an N-CoR-specific antibody affinity column and then gel filtration. We can

check to ensure that we have purified the complex and exactly what components are present by mass spectrometry and Western blotting for the various proteins of the complex.

Once we have isolated the N-CoR/SMRT complex, we will compare its cleavage with wild type caspase-3 and our half-labeled hybrid construct through time course analysis. In this experimental setup, we are not able to monitor cleavage events of single complexes as we were able to do with the gold nanoparticle system. Instead, we must track the overall level of uncleaved components of the complex. We will do this by checking the levels of our proteins of interest by Western blot at 15 minute intervals. Since the half-labeled hybrid is not able to cleave substrates in a processive fashion, we expect to see slower cleavage of substrates in complexes for this construct. If the cleavage of any component is drastically slowed or prevented in the case of the non-processive enzyme, this would suggest that either the order of cleavage events or the coordinated cutting of caspase targets is necessary for efficient dismantling of the N-CoR/SMRT complex.

For the second half of this study, we will transfect cells with tagged components of the N-CoR/SMRT complex, and use a TAP-affinity tag to purify the complex. Clearly, the use of affinity tags on the complex may preclude certain components from associating. To get around this, we can tag different components of the complex and compare the composition of the complex we pull down to the untagged complex that was isolated above. The advantage of this method is that it allows us to mutate the tagged component of interest. Since we are isolating the complex through identification of the tagged protein, we should not have to worry about endogenous levels of wild type protein in this context. This experimental setup will allow us to ask more specific questions as to the importance of cleaving specific sites in the complex.

For example, this method will allow us to tag the N-CoR protein, mutate out a specific caspase cleavage site, and then see if the cleavage of remaining sites in N-CoR or the complex is affected. If we find that the cleavage of a second site is slowed or blocked, what would this suggest? It could mean that the cleavage of the first site is necessary for the second site to be exposed in the complex. Another possible explanation is that the action of a processive protease is required for efficient cutting of the second site. If this is the case, then we should see still a difference in the cleavage of the second site even when the first site is not mutated when we compare wild type caspase-3 activity to that of our half-labeled construct. By making different tagged constructs with mutations of the various cleavage sites, we may be able to determine a possible order of cleavage events for dismantling of the complex.

In conclusion, the caspases are unusual among proteases in adopting a dimer conformation in their active state, and caspase-1 is unique among the caspases in demonstrating positive cooperativity. Recent experimental evidence suggests that caspases may preferentially target substrates in protein complexes. The experiments described above aim to determine whether there is functional relevance for a dimer protease in the cooperative and processive cleavage of substrates in complexes.

4.4 Searching for an endogenous allosteric caspase-1 inhibitor

Though recent studies have shed light on the regulation of caspase-1 before it is activated from the zymogen form, little is known about how caspase-1 activity is regulated after activation. Unlike caspase-7 that can be inhibited by XIAP once activated, there are few known examples of natural inhibitors of caspase-1 (Young, Sukhova et al. 2000). All of the known caspase-1 inhibitors, such as COP, ICEBERG, PI-9, and pyrin seem to act intracellularly. They are

thought to either regulate IL-1β production by inhibiting the inflammatory pathway before procaspase-1 is processed to its active form by inhibiting its recruitment to inflammasomes, or act by interfering with caspase-1 and inflammasome activity (Church, Cook et al. 2008).

The end result of the caspase-1/IL-1β activation pathway is the secretion of IL-1β, which then acts as an inflammatory cytokine towards other cells. It is known that caspase-1 is also secreted from the cell along with IL-1β after processing (MacKenzie, Wilson et al. 2001; Andrei, Margiocco et al. 2004; Ferrari, Pizzirani et al. 2006). This raises the question as to how the secreted, active caspase-1 is then regulated outside of the cell. Conceivably, it would not be ideal to have an active protease in the extracellular space for very long. Thus, it is reasonable to suspect that an endogenous caspase-1 inhibitor may exist in the extracellular compartment, especially in the context of inflammatory stimulation and IL-1β secretion by immune cells.

In order to investigate this possibility, we decided to probe for a natural regulator of activated caspase-1 in the media of cells that have been stimulated to produce IL-1β. The THP-1 cell line is derived from a patient with acute monocytic leukemia (Tsuchiya, Yamabe et al. 1980). These monocytes are precursor immune cells that can be induced to differentiate into macrophages. Stimulation of these cells with bacterial lipopolysaccharide followed by ATP leads to the secretion of IL-1β into the cell culture media. We collected this conditioned media from stimulated THP-1 cells and then fractionated using strong cation exchange chromatography (SCX). Interestingly, we observed a “peak” of inhibitory activity among the fractions collected from SCX (Fig 4.3, left). These fractions were able to reduce caspase-1 enzyme activity by up to 80% in a dose-dependent manner (Fig 4.3, right).

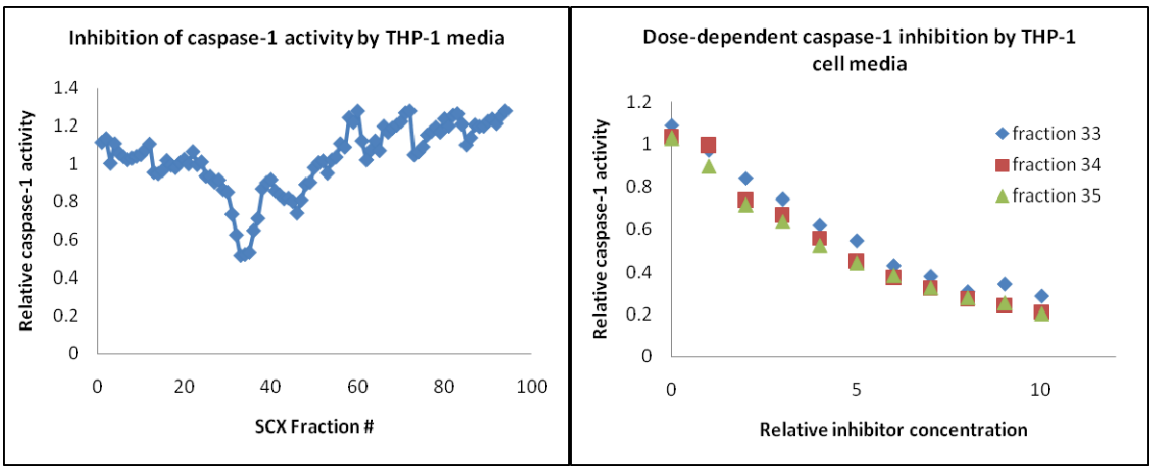

Figure 4.3. Inhibition of caspase-1 by media from stimulated THP-1 cells. (Left) Screening of inhibitory activity of fractionated THP-1 media against caspase-1 identified a "peak" of lowered activity centered at fraction 34. **(Right)** Titration of fractions 33, 34, and 35 against caspase-1 demonstrates dose-dependent inhibition of caspase-1 activity.

We have not further characterized this peak to determine if it is a protein or small molecule, and clearly it would be a challenge to do so. However, the tools we have developed to probe caspase-1 allostery may serve us well in trying to identify the mechanism of action of this putative endogenous inhibitor and possibly to isolate it as well. For example, we could test this inhibitor against our half-labeled hybrid caspase-1 construct in order to determine whether it is able to bind and inhibit the active form of the enzyme. Failure to do so would suggest that it may be trapping the caspase-1 molecule in the inactive conformation, and therefore could be an allosteric inhibitor. We could test for covalent modification by isolating caspase-1 that is secreted from THP-1 cells using our conformation-specific antibodies and then characterizing the protein by mass spectrometry. Even if the putative inhibitor is not a covalent modifier of caspase-1, it may be able to compete for binding with the conformation-specific antibodies, and this too could suggest which conformational state the inhibitor is binding to.

Other avenues for identifying this inhibitor exist. One possible candidate is proteolytic fragments from processing of pro-IL-1β. It was recently reported that the intersubunit linker of

caspase-1 binds in the dimer interface before it is cleaved off. This raises the possibility that proteolytic fragments from the intersubunit linker or even the N-terminal prodomains are secreted along with caspase-1 and IL-1β and that these fragments inhibit caspase-1 activity in the extracellular space. Yet another possibility is that caspase-1 is inactivated by reactive oxygen species at the allosteric cysteine-331, or active site cysteine-285. Several reports have suggested that nitric oxide may regulate caspase-3 by thiol nitrosylation and a similar mechanism may exist for caspase-1 (Matsumoto, Comatas et al. 2003; Mitchell and Marletta 2005). The recent development of robust docking algorithms for metabolites provides another avenue to search for a natural allosteric ligand (Kalyanaraman, Bernacki et al. 2005). These methods would allow us to dock metabolites into caspase-1 that may bind to either the active or allosteric sites of caspase-1. We could then test top hits of a docking screen *in vitro* to determine if we see inhibition at physiologically relevant concentrations. Finding a natural regulator would greatly advance our understanding of the biology of the inflammatory caspases, just as discovery and characterization of the XIAP family were a breakthrough for understanding the regulation of the apoptotic caspases.

4.5 Impact and Future Studies

The studies presented in this dissertation provide a framework for developing new approaches for trapping allosteric transitions and conformational states in proteins using small molecules and site-directed mutagenesis. Such techniques allow for these states to be more clearly studied in various settings. Extending these methods to other enzyme systems will allow us to further define the internal allosteric circuitry in enzymes that support conformational states.

4.6 Experimental Procedures

4.6.1 Expression and purification of recombinant caspase-1 and caspase-7

Recombinant caspase-1 and caspase-7 were prepared by expression in *Escherichia coli (E. coli)* as insoluble inclusion bodies followed by refolding (Romanowski, Scheer et al. 2004; Scheer, Wells et al. 2005). Site-directed mutagenesis was performed using the QuikChange Site-Directed Mutagenesis Kit from Stratagene (La Jolla, CA). Caspase subunits were expressed separately in *E. coli* BL21(DE3) Star cells (Invitrogen). Cells were harvested following induction of a log phase culture with 1mM IPTG for 4 h at 37°C and then disrupted with a microfluidizer. The inclusion body pellets were isolated by centrifugation of lysate for 20 min at 4°C. Pellets were washed twice with 50 mM HEPES (pH 8.0), 300 mM NaCl, 1 M guanidine-HCl, 5 mM DTT, and 1% Triton X-100, and washed two more times with the same buffer without the detergent. The washed inclusion body pellets were solubilized in 6 M guanidine-HCl and 20 mM DTT, and stored frozen at -80°C.

Refolding of caspase was done by combining guanidine-HCl-solubilized large and small subunits (10mg of large subunit and 20mg of small subunit) in a 250 mL beaker, followed by rapid dilution with 100 mL of 50 mM HEPES (pH 8.0), 100 mM NaCl, 10% sucrose, 1 M nondetergent sulfobetaine 201 (NDSB-201), and 10 mM DTT. Renaturation proceeded at room temperature for 6 h. Samples were centrifuged at 16,000 g for 10 minutes to remove precipitate, and then dialyzed overnight at 4°C against 50 mM sodium acetate (pH 5.9), 25 mM NaCl, 5% glycerol, and 4 mM DTT. Dialyzed protein was purified by cation exchange chromatography using a pre-packed 5 mL HiTrap SP HP column (GE Healthcare Bio-sciences Corp, Piscataway, NJ). Protein was eluted using a linear gradient of 0-1.0 M NaCl over 20 min in

a buffer containing 50 mM sodium acetate (pH 5.9) and 5% glycerol. Peak fractions were pooled and β-ME was added to a concentration of 1mM before samples were stored frozen at -80°C.

4.6.2 Enzyme kinetic analysis

For kinetic analysis of caspase-1, protein was buffer exchanged using a NAP-5 Column (Amersham) into assay buffer containing 50 mM HEPES (pH 8.0), 50 mM KCl, 200 mM NaCl, 10 mM DTT, 0.1% 3-[(3-cholamidopropyl)dimethylammonio]-1-propanesulfonate (CHAPS). Kinetic analysis of caspase-7 was performed in buffer containing 50 mM HEPES (pH 7.4), 50 mM KCl, 0.1 mM EDTA, 1 mM DTT and 0.1% CHAPS. Steady-state kinetic analysis was done by titrating enzyme with fluorogenic tetrapeptide substrate (Ac-WEHD-AFC for caspase-1 constructs and Ac-DEVD-AFC for caspase-7 constructs; Axxora, San Diego, CA) typically from 200 μM to 0.25 μM. The enzyme concentration was set to 50 nM for all variants. Kinetic data was collected for a 10 min time course using a Spectramax M5 microplate reader (Molecular Devices, Sunnyvale, CA) with excitation, emission, and cutoff filters set to 365 nm, 495 nm, and 435 nm, respectively.

Kinetic constants V_{max}, K_M, and the Hill coefficient (n_{Hill}) were calculated using GraphPad prism. The initial velocity (*v)*, measured in relative fluorescence units per unit time, was plotted versus the logarithm of substrate concentration. The model used to fit the data is a sigmoidal does-response curve with variable slope, and from this model all three kinetic constants were derived. The general equation of this model is Y = Bottom + (Top-Bottom)/(1+10^((LogEC_{50}-X)*HillSlope)), where Y is the initial velocity, X is the logarithm of the substrate concentration, and Top, Bottom, EC_{50} (K_M), and Hill Slope are free parameters fit to the data. A standard curve using pure AFC product was used to convert relative fluorescence units to units of concentration (μM). In determining kinetic constants for caspases we observed that at saturating substrate

concentrations, the enzyme exhibited decreasing activity as substrate concentration increased, most likely due to substrate inhibition. In order to correctly fit our data using non-linear regression, data points exhibiting product inhibition were excluded.

4.6.3 THP-1 cell culture and media fractionation

THP-1 cells (Tsuchiya, Yamabe et al. 1980) were grown to a density of 5 X 10^5 cell/ml and then differentiated by treatment with 100 nM 12-*O*-tetradecanoylphorbol-13-acetate (TPA) for four hours in 225 cm^2 tissue culture-treated plates. To induce IL-1β secretion, cells were primed with 1 μg/ml lipopolysaccharide (LPS, from *Escherichia coli* O55:B5, Sigma) for 2 hours followed by activation with 5 mM ATP for 2 hours. The media was then collected, pooled and stored at -80°C until ready for fractionation.

Two liters of pooled cell culture media from activated THP-1 cells were fractionated by anion exchange chromatography using a pre-packed 5 mL HiTrap Q HP column (GE Healthcare Bio-sciences Corp, Piscataway, NJ). Fractions were collected over a 10-column volume gradient from 0-1.0 M NaCl in buffer containing 20 mM Tris, pH 8.0 and 5% glycerol. The flow through during Q HP column load was collected and loaded on a second column for fractionation by cation exchange chromatography using a pre-packed 5 mL HiTrap SP HP column (GE Healthcare Bio-sciences Corp, Piscataway, NJ). Fractions were collected over a linear gradient of 0-1.0 M NaCl over 10 column volumes in buffer containing 50 mM sodium acetate (pH 5.9) and 5% glycerol.

4.6.4 Kinetic analysis of caspase-1 inhibition by fractionated THP-1 media

The inhibitor potential of fractionated media was tested by adding 5 µL of a fraction to 40 µL of caspase-1 in assay buffer (50 mM HEPES (pH 8.0), 50 mM KCl, 200 mM NaCl, 10 mM DTT, 0.1% CHAPS). After thirty minute incubation, caspase-1 activity was assayed by adding 5 µL of solution containing Ac-WEHD-AFC substrate (Axxora, San Diego, CA) to give final concentrations of 50 nM caspase-1 and 25 µM substrate.

Dose-dependent inhibition by fractionated media was performed by adding 0-10 µL of a fraction sample in 1 µL increments to 45 µL of caspase-1 in assay buffer (described above). After thirty minute incubation, caspase-1 activity was assayed by adding 5 µL of solution containing Ac-WEHD-AFC substrate (Axxora, San Diego, CA).

4.7 References

Andrei, C., P. Margiocco, et al. (2004). "Phospholipases C and A2 control lysosome-mediated IL-1 beta secretion: Implications for inflammatory processes." Proc Natl Acad Sci U S A **101**(26): 9745-50.

Bolden, J. E., M. J. Peart, et al. (2006). "Anticancer activities of histone deacetylase inhibitors." Nat Rev Drug Discov **5**(9): 769-84.

Church, L. D., G. P. Cook, et al. (2008). "Primer: inflammasomes and interleukin 1beta in inflammatory disorders." Nat Clin Pract Rheumatol **4**(1): 34-42.

Escaffit, F., O. Vaute, et al. (2007). "Cleavage and cytoplasmic relocalization of histone deacetylase 3 are important for apoptosis progression." Mol Cell Biol **27**(2): 554-67.

Ferrari, D., C. Pizzirani, et al. (2006). "The P2X7 receptor: a key player in IL-1 processing and release." J Immunol **176**(7): 3877-83.

Kalyanaraman, C., K. Bernacki, et al. (2005). "Virtual screening against highly charged active sites: identifying substrates of alpha-beta barrel enzymes." Biochemistry **44**(6): 2059-71.

Karagianni, P. and J. Wong (2007). "HDAC3: taking the SMRT-N-CoRrect road to repression." Oncogene **26**(37): 5439-49.

MacKenzie, A., H. L. Wilson, et al. (2001). "Rapid secretion of interleukin-1beta by microvesicle shedding." Immunity **15**(5): 825-35.

Maggiora, L. L., C. W. Smith, et al. (1992). "A general method for the preparation of internally quenched fluorogenic protease substrates using solid-phase peptide synthesis." J Med Chem **35**(21): 3727-30.

Mahrus, S., J. C. Trinidad, et al. (2008). "Global Sequencing of Proteolytic Cleavage Sites in Apoptosis by Specific Labeling of Protein N Termini." Cell.

Matayoshi, E. D., G. T. Wang, et al. (1990). "Novel fluorogenic substrates for assaying retroviral proteases by resonance energy transfer." Science **247**(4945): 954-8.

Matsumoto, A., K. E. Comatas, et al. (2003). "Screening for nitric oxide-dependent protein-protein interactions." Science **301**(5633): 657-61.

Mitchell, D. A. and M. A. Marletta (2005). "Thioredoxin catalyzes the S-nitrosation of the caspase-3 active site cysteine." Nat Chem Biol **1**(3): 154-8.

Reinhard, B. M., S. Sheikholeslami, et al. (2007). "Use of plasmon coupling to reveal the dynamics of DNA bending and cleavage by single EcoRV restriction enzymes." Proc Natl Acad Sci U S A **104**(8): 2667-72.

Romanowski, M. J., J. M. Scheer, et al. (2004). "Crystal structures of a ligand-free and malonate-bound human caspase-1: implications for the mechanism of substrate binding." Structure **12**(8): 1361-71.

Scheer, J. M., J. A. Wells, et al. (2005). "Malonate-assisted purification of human caspases." Protein Expr Purif **41**(1): 148-53.

Sonnichsen, C., B. M. Reinhard, et al. (2005). "A molecular ruler based on plasmon coupling of single gold and silver nanoparticles." Nat Biotechnol **23**(6): 741-5.

Tsuchiya, S., M. Yamabe, et al. (1980). "Establishment and characterization of a human acute monocytic leukemia cell line (THP-1)." Int J Cancer **26**(2): 171-6.

Yoon, H. G., D. W. Chan, et al. (2003). "Purification and functional characterization of the human N-CoR complex: the roles of HDAC3, TBL1 and TBLR1." EMBO J **22**(6): 1336-46.

Young, J. L., G. K. Sukhova, et al. (2000). "The serpin proteinase inhibitor 9 is an endogenous inhibitor of interleukin 1beta-converting enzyme (caspase-1) activity in human vascular smooth muscle cells." J Exp Med **191**(9): 1535-44.

Publishing Agreement

It is the policy of the University to encourage the distribution of all theses, dissertations, and manuscripts. Copies of all UCSF theses, dissertations, and manuscripts will be routed to the library via the Graduate Division. The library will make all theses, dissertations, and manuscripts accessible to the public and will preserve these to the best of their abilities, in perpetuity.

Please sign the following statement:

I hereby grant permission to the Graduate Division of the University of California, San Francisco to release copies of my thesis, dissertation, or manuscript to the Campus Library to provide access and preservation, in whole or in part, in perpetuity.

Deborah Dilley

Author Signature

6/21/10

Date